FEMS Microbiology Ecology, 2025, 101, fiaf109
DOI: 10.1093/femsec/fiaf109
Advance access publication date: 25 October 2025
Research Article

Temporal and spatial dynamics of microbial communities and greenhouse gas flux responses to experimental flooding in riparian forest soils

Kristel Reiss[1,*], Ülo Mander[1], Maarja Öpik[2], Siim-Kaarel Sepp[2,3], Kärt Kanger[1], Thomas Schindler[1], Kaido Soosaar[1], Mari Pihlatie[4,5], Klaus Butterbach-Bahl[6], Anuliina Putkinen[4,5], Ülo Niinemets[7], Mikk Espenberg[1]

[1]Institute of Ecology and Earth Sciences, University of Tartu, Vanemuise 46, Tartu 51003, Estonia
[2]Institute of Ecology and Earth Sciences, University of Tartu, J. Liivi 2, Tartu 51003, Estonia
[3]Netherlands Institute of Ecology (NIOO-KNAW), Droevendaalsesteeg 10, 6708 PB Wageningen, The Netherlands
[4]Department of Agricultural Sciences, University of Helsinki, PO Box 56, Helsinki 00014, Finland
[5]Institute for Atmospheric and Earth System Research, Faculty of Agriculture and Forestry, University of Helsinki, PO Box 56, Helsinki 00014, Finland
[6]Department of Agroecology, Land-CRAFT, Center for Landscape Research in Sustainable Agricultural Futures, Aarhus University, Blichers Allé 20, 8830 Tjele, Denmark
[7]Chair of Crop Science and Plant Biology, Estonian University of Life Sciences, Kreutzwaldi 1, 51006 Tartu, Estonia
*Corresponding author. Institute of Ecology and Earth Sciences, University of Tartu, Vanemuise 46, Tartu 51003, Estoni. E-mail: kristel.reiss@ut.ee
Editor: Tillmann Lueders

Abstract

Extreme rainfall and flooding are expected to increase in Northern subboreal habitats, altering soil hydrology and impacting greenhouse gas (GHG) fluxes by shifting redox potential and microbial communities as soils transition from aerobic to anaerobic conditions. This study examined the effects of a 2-week growing-season flash flood on bacterial, archaeal, and fungal communities and microbial processes driving CH_4 and N_2O fluxes in riparian alder (*Alnus incana*) forests. Flooding reduced soil nitrate accumulation as determined by quantitative polymerase chain reaction and promoted dinitrogen-fixing, *nifH* gene-carrying bacteria like *Geomonas*. Sequencing data showed that anaerobic bacteria (*Oleiharenicola*, *Pelotalea*) increased during the flood, while N_2O emissions declined, indicating a shift towards complete denitrification to N_2. However, drier patches within the flooded area emitted N_2O, suggesting nitrification or incomplete denitrification. A diverse arbuscular mycorrhizal community was detected, including genera *Acaulospora*, *Archaeospora*, *Claroideoglomus*, *Diversispora*, and *Paraglomus*. Flooding increased the abundance of the fungal genera *Naucoria*, *Russula*, and *Tomentella* and the family *Thelephoraceae*, which symbiotically support alder trees in nitrogen uptake and carbon sequestration. Microtopographic differences of 0.3–0.7 m created spatial variability in GHG emissions during flooding, with some waterlogged areas emitting CH_4, while others enhanced CH_4 oxidation (determined by FAPROTAX) and promoted nitrification-driven N_2O emissions in drier, elevated zones. We conclude that flash flooding during the active growing season significantly affects nitrogen-fixing and nitrifying microbes and alters symbiotic fungal community composition, creating spatial variability in GHG emissions.

Keywords: arbuscular mycorrhizal fung; bacteria; fungi; methane; microtopography; nitrous oxide

Introduction

The International Panel on Climate Change (IPCC) reported that atmospheric carbon dioxide (CO_2) levels are the highest in 2 million years, with methane (CH_4) and nitrous oxide (N_2O) concentrations also significantly rising (Reed et al. 2011, IPCC 2021). These increases are associated with climate warming and a rising frequency of extreme climate events, such as intense rainfall and floods (IPCC 2021). Such extremes alter soil hydrological regimes (Schindler et al. 2020, Furtak and Wolińska 2023) and impact microbial communities, including their diversity and function (Unger et al. 2009, Hutchins et al. 2019). The changes in soil prokaryotic and fungal abundances and communities are often associated with shifts in N_2O (Zhang et al. 2021a, Espenberg et al. 2018) and CH_4 (Wang et al. 2023, Yang et al. 2024) fluxes.

Riparian ecosystems, which act as periodically flooded buffer zones (Naiman et al. 2010), can help mitigate these climate-driven changes. They intercept the excess nutrients transported via flood and soil runoff (Peter et al. 2012, Lyu et al. 2021), bind nutrients with organic matter (OM) (Lidman et al. 2017), and retain pollutants (Riis et al. 2020). Their nutrient-binding capacity depends on factors, such as soil type (Pinay et al. 1995), topography (Adhikari et al. 2018), buffer width (Lyu et al. 2021, Graziano et al. 2022, Mander et al. 1997), vegetation (Petersen et al. 2020, Tolkkinen et al. 2020), hydrology (Tolkkinen et al. 2020), and groundwater level fluctuations (Hefting et al. 2004). Riparian forests also provide aerobic and anaerobic microbial habitats that drive soil biogeochemical processes involved in the production and consumption of greenhouse gases (GHGs) such as CH_4 and N_2O (Annala et al. 2022). Additionally, the impact of flooding on subboreal vegetation depends significantly on its duration and timing (Sarneel et al. 2019). In riparian areas, flooding typically occurs in spring and autumn when vegetation is mainly dormant and exhibits reduced physiological activity. However, intense rainfall can also cause flooding during the peak growing season, potentially

Received 19 June 2025; **revised** 28 September 2025; **accepted** 21 October 2025

resulting in severe damage to vegetation (Van Eck et al. 2006). European riparian areas total ~91 144 km^2, with northern countries like Finland and Estonia having the highest relative cover (Clerici et al. 2013). In North-Eastern Europe, grey alder (*Alnus incana* (L.) Moench) is common in riparian zones (Lõhmus et al. 1996, Aosaar et al. 2012, Uri et al. 2014) due to its adaptation to high soil moisture conditions (Johansson 1999).

Studies in riparian areas show that flooding and higher groundwater levels can increase CH_4 emissions from grey alder (*A. incana*) stands (Soosaar et al. 2011, Mander et al. 2015). Net CH_4 release occurs in soils where methanogenic archaea, the final recipients of substrates originating from OM fermentation, outcompete methanotrophs in their activity (Guerrero-Cruz et al. 2021). Emissions occur mainly through diffusion, bubbles, and mass flow through plant aerenchyma (Le Mer and Roger 2001). Oxidation of CH_4 occurs primarily by aerobic methanotrophs (Le Mer and Roger 2001) but can also take place anaerobically (Boetius et al. 2000) via nitrite-dependent anaerobic methane oxidation (n-damo) by bacteria from the NC10 phylum (Ettwig et al. 2009), or via the archaeal domain (e.g. *Methanoperedenaceae*), oxidizing CH_4 by reverse methanogenesis (Cui et al. 2015). CH_4 emissions vary seasonally, with warmer temperatures promoting methanogenic activity (Li et al. 2023). Riparian areas are traditionally known as CH_4 sinks, but the increased frequency of long-term and short-term flooding may alter them from sinks to CH_4 sources in periods of prolonged, flooding-induced soil anaerobiosis (Jacinthe 2015). Additionally, higher precipitation and, thus, soil moisture reduce soil's ability to oxidize CH_4, leading to increased emissions (Guo et al. 2023).

Flooding can also increase N_2O emissions, with higher emissions observed after short-term flooding (Jacinthe et al. 2012) or immediately after rewetting (Harris et al. 2021). N_2O is mainly a by-product of nitrification or denitrification (Hallin et al. 2018) but may also be emitted through dissimilatory NO_3^- reduction to ammonia (NH_3^+) (DNRA) under certain conditions (Rütting et al. 2011, Mania et al. 2014). In riparian zones, the importance of denitrification has been highlighted (Mander et al. 2014). Additionally, complete nitrifiers known as comammox can oxidize NH_3^+, but the potential for N_2O production remains unclear (Koch et al. 2019). In organic-rich soils, N_2O emissions are influenced by temperature, soil moisture, NO_3^- concentration (Pärn et al. 2018), and vegetation (Hernandez and Mitsch 2006). In grey alder forests, biological dinitrogen (N_2) fixation is another key process, converting N_2 to NH_4^+, accessible to plants. It has been shown that soil water content is an important factor in N_2 fixation, and decreased soil water content can decrease biological N_2 fixation (Whiteley and Gonzalez 2016, Zhang et al. 2020). Grey alder forms a symbiotic relationship with N-fixing bacteria from the genus *Frankia* (Franche et al. 2009, Sellstedt and Richau 2013). Increased water availability has also been shown to result in increased N_2 fixation rates by a diverse group of free-living N_2-fixers (Reed et al. 2011).

In addition to the prokaryotic microbes, changes in the fungal community can significantly affect ecosystem carbon (C) cycling and storage (Orwin et al. 2011). Fungi are essential in several ecosystem processes, including C sequestration (Clemmensen et al. 2013), and decomposition of litter (Kubartová et al. 2009) and organic C (Treseder and Lennon 2015). Most plants form symbiotic relationships with fungi, which transfer nutrients like nitrogen (N) and phosphorus (P) from soil to plants (van Der Heijden et al. 2015) in exchange for carbohydrates and fatty acids (Diagne et al. 2020). Fungi also play an essential role in the N cycle (Gui et al. 2021, Huaisong et al. 2024). Arbuscular mycorrhizal fungi (AMF) can influence the abundance of genes involved in soil N cycle, indirectly affecting N_2O emissions (Okiobe et al. 2022, Qiu et al. 2022). In addition, N_2O can be produced through fungal denitrification, a process in which fungi reduce nitrite (NO_2^-) to nitrous oxide N_2O (Shoun et al. 2012). The phylum *Ascomycota* includes fungi that produce N_2O (Mothapo et al. 2015), such as certain species of *Fusarium* (Lin et al. 2024).

Riparian areas are complex ecosystems, where aerobic and anaerobic microbial C and N processes can cooccur, making it crucial to study both together and link them to temporal changes in soil redox potentials (Espenberg et al. 2024). While many studies have explored the effects of environmental factors such as rainfall or temperature on GHG emissions, the impact of ecological disturbances, such as flooding on microbial processes and community structures requires further analysis (Cavicchioli et al. 2019). There are particularly few studies on the impact of growing season flooding on riparian microbial communities and associated changes in GHG emissions. This study investigated how short-term flooding during the growing season influences the soil microbiome and the importance of flooding periods in shaping soil microbial N and C cycles and associated GHG production, oxidation, and emission processes in a riparian alder forest. It focused on how soil bacteria, fungi, and AMF communities relate to physicochemical characteristics and soil CH_4 and N_2O emissions during short-term flooding.

The study hypothesized that: (1) experimental flooding during the plant growing season decreases bacterial and fungal diversity; (2) flooding-dependent changes in the microbiome are responsible for decreases in N_2O emissions and increases in CH_4 emissions after flooding; and (3) rapidly changing soil moisture content and induced soil anaerobiosis mainly affects nitrifying microbial communities, including microbes mediating the complete ammonia oxidation (comammox) process.

Materials and methods

Site description, experimental set-up, and soil sampling

The experimental site (58° 17′ N; 27° 17′ E, 36 m asl) is in a riparian forest near the Kalli River in Agali, Tartu County, Estonia (Fig. S1). The area is situated on gley soil, and the thickness of the raw humus horizon at the study site ranges from 15 to 20 cm (Mander et al. 2022). The site is a former agricultural land dominated by a 40-year-old grey alder [*A. incana* (L.) Moench] forest, and the understory includes bird cherry (*Prunus padus* L.), meadowsweet [*Filipendula ulmaria* (L.) Maxim.], and raspberry (*Rubus idaeus* L.) The experimental site was divided into a control plot (CP) and an experimental plot, i.e. the flooded plot (FP). The FP measured ca 40 m × 40 m, and the CP was ca 20 m × 20 m, separated by a natural 1-m dyke. To mimic an intensive rainfall creating a runoff, each day during the flooding (14 days), 55–70 m^3 of water was transported to the FP by a fire truck.

The experiment consisted of four intensive measuring periods and, and each period consisted of two sampling campaigns, except the final sampling period (POSTPOST), which consisted of one campaign (altogether seven sampling campaigns). Soil samples were collected during the preexperimental period (PRE) on 25 or 26 July and 7 August 2017, during the artificial flooding period (EXP) on 16 and 21 August 2017 (the 8th and 13th day of the flood), and during the postexperimental period (POST) on 11 or 12 September and 7 November 2017 (21 or 22 days after the flooding and 78 days after the flooding, respectively). The final soil samples were collected the following year, on 15 August 2018 (POSTPOST).

During each sampling campaign, 12 samples were collected: 8 from the FP and 4 from the CP. We designed the study so that the flooded and CPs were as close together as possible to ensure comparability, while ensuring that floodwater did not affect the CP. Sampling locations within plots were randomly selected. The soil samples were taken at a depth of 0–10 cm with a spade from the vicinity of the grey alder trees. Samples were collected following a random sampling strategy, where each composite sample was formed by pooling three subsamples from the same soil layer. A total of 84 composite samples were collected. The samples were stored in a refrigerator (+4°C) for chemical and in a freezer (−20°C) for microbiological analyses. A more detailed description of the site, experimental setup, and sampling procedures is available in Schindler et al. (2020).

Physiochemical analyses and GHG emission analyses

Soil temperature, water content and soil moisture were measured during the experiment at 0–10 cm depth. Soil pH_{KCl}, total nitrogen (N%), NO_3^-, NH_4^+, total P, potassium (K), calcium (Ca), magnesium (Mg), and OM contents were measured using the standard protocol (APHA-AWWA-WEF 2005). Soil N_2O and CH_4 fluxes were measured 12 times daily with 12 automated chambers, each covering 0.16 m^2 forest floor and placed near representative grey alder trees. A Picarro G2508 (Picarro Inc., USA) gas analyser with cavity ring-down spectroscopy technology was used to monitor GHG gas concentrations. A detailed description of the physico-chemical analyses and GHG measurements can be found in Schindler et al. (2020).

Soil DNA extraction

The PowerSoil® DNA Isolation Kit (Qiagen, USA) was used to extract DNA from the soil samples (0.25 g), following the manufacturer's protocol. The samples were homogenized for 20 s at 5000 r/m using a Precellys® 24 homogenizer (Bertin Technologies SAS, France). The quantity and quality of the DNA were assessed using a spectrophotometer Infinite M200 (Tecan Trading AG, Switzerland). The extracted DNA was stored at −20°C until further analysis.

Quantification of gene copies using quantitative polymerase chain reaction

Functional estimates of microbial biogeochemical processes were based on quantifying established functional marker genes using real-time quantitative polymerase chain reaction (qPCR). The qPCR analyses were performed using a Rotor-Gene Q thermocycler (Qiagen, USA). The 10 μl reaction mixture for amplification contained 5 μl of Maxima SYBR Green Master Mix (Thermo Fisher Scientific Inc., USA), optimized forward and reverse primers, 1 μl of isolated sample DNA, and sterile distilled water. Measurements with qPCR were performed in triplicate for each sample, and negative controls were included for each measurement.

Rotor-Gene Series Software v 2.0.2 was used to analyse the amplification and melting curves of the samples, and LinReg PCR v 2020.0 was used to consider the amplification efficiencies of the samples. Gene copy numbers were calculated using the corresponding standard curve for each marker gene, and gene abundances were expressed as the number of gene copies per gram of dry matter (copies/gDM). The qPCR standard curves were constructed using plasmids containing cloned gene fragments (Eurofins Genomics, Germany). Standard curves were then generated from serial dilutions of these plasmid DNA stock solutions, ranging from 10^9 to 25 copies per 10 μl of qPCR reaction mixture, depending on the target gene. The exact dilution series used are reported in Table S1.

Functional genes related to the N cycle were quantified, using primers nirSCd3 and nirSR3cd (Kandeler et al. 2006) for *nirS*, nirK876 and nirK1040 (Hallin and Lindgren 1999) for *nirK*, nosZ2F and nosZ2R (Henry et al. 2006) for *nosZ* clade I (*nosZI*), nosZ-II-F and nosZ-II-R (Jones et al. 2013) for *nosZ* clade II (*nosZII*) (prokaryotic denitrification), FnirK-F3 and FnirK-R2 (Chen et al. 2016) for fungal *nirK* (fungal denitrification), amoA-1F and amoA-2R (Rotthauwe et al. 1997) for bacterial and CrenamoA 23F and CrenamoA 616R (Tourna et al. 2008) for archaeal *amoA* (nitrification), comamoA AF and comamoA SR (Wang et al. 2018) for COMAMMOX *amoA* (complete ammonia oxidation), 6RF and 6R (Takeuchi 2006) for *nrfA* (DNRA), and Ueda19F and Ueda407R (Ueda et al. 1995) for *nifH* (nitrogen fixation). For CH_4 cycle processes the following primers were used: mcrA-F and mcrA-R (Espenberg et al. 2016) for *mcrA* (methanogenesis), A189F and Mb661R for *pmoA* (methanotrophy), and pq2F and pq2R for (Ettwig et al. 2009) n-damo-specific 16S rRNA (nitrite/nitrate-dependent anaerobic CH_4 oxidation) genes. All primer sets for target genes, amplification efficiencies, optimized primer concentrations, and optimized qPCR programs are listed in Table S1.

Preparation of DNA libraries, sequencing, and data processing

We used a soil metabarcoding approach to characterize the bacterial, fungal, and more specifically, the AMF community. Total environmental DNA was extracted from bulk soil samples (not specifically picked from roots) as stated above, and specific marker genes were subsequently amplified from the DNA extracts. Sequencing was performed using bacterial 16S rRNA gene primers 515F and 806rB (Caporaso et al. 2011), general fungal-specific Internal Transcribed Spacer (ITS) region primers fITS7o, fITS7, and ITS4 (White et al. 1990, Ihrmark et al. 2012, Kohout et al. 2014), and AMF-specific SSU rRNA gene primers WANDA and AML2 (Lee et al. 2008, Dumbrell et al. 2011). Sequencing was conducted on the Illumina MiSeq platform with 2 × 250 bp and 2 × 300 bp chemistry for bacteria and all fungi or AMF, respectively (Illumina, California, USA). Amplicon-based polymerase chain reaction (PCR) and sequencing were carried out by Asper Biogene OÜ (Tartu, Estonia). Although the universal prokaryotic 16S rRNA primers 515F and 806rB capture some of the archaeal community, they have been shown to severely underestimate its diversity (Bahram et al. 2019). Hence, we did not include archaeal sequences in downstream analysis.

The DADA2 package (Callahan et al. 2016) was used to aggregate demultiplexed raw sequencing reads into exact amplicon sequence variants (ASV). Primer sequences were removed from bacterial and fungal fragments using the cutadapt program (Martin 2011). Due to ambiguous nucleotide bases (Ns) and very short sequences, filtering was repeated after primer removal using the *filterAndTrim()* function from the DADA2 package, with MaxN = 0, truncQ = 2, minLen = 50, and rm.phix = TRUE. After filtering, the sequences were assembled using the *makeSequenceTable()* function, and taxonomy was added using the *assignTaxonomy()* function from the DADA2 package. The SILVA v138.2 database (Quast et al. 2013) was used for bacterial taxonomy assignment. The SILVA database taxonomy was formatted to fasta files (Callahan 2024) and used in the DADA2 workflow. The UNITE database (Kõljalg et al. 2020) was used for fungal taxonomy assignment. The MaarjAM database (Öpik et al. 2010) was used for AMF taxonomy assignment (identification to match against virtual taxa, VT).

The software 'R version 4.3.2' and 'RStudio 2022.12.0' were used for data processing and bioinformatic analyses. Bacterial ASV, fungal ASV, and AMF VT data, samples, and taxonomy tables were used to create *phyloseq* objects with the Phyloseq package (McMurdie and Holmes 2013). In the *phyloseq* object, the relative abundance was calculated using the *transform_sample_counts()* function from the Phyloseq package. The Phyloseq functions *estimate_richness()* and *plot_richness()* were used to estimate bacterial and fungal diversity (McMurdie and Holmes 2013). The Shannon (H') index was calculated to assess α-diversity (Xia and Sun 2023). The Shannon (H') index is calculated using the following formula: $H' = -\sum_{i=1}^{S} p_i \ln(p_i)$, where p_i is the proportional abundance of genera i, S is the number of unique genera, and ln is the natural logarithm (Oksanen 2024).

In addition, bacterial ASV data were functionally annotated using the FAPROTAX database (Louca et al. 2016) to estimate the potential biogeochemical functions of the bacterial community based on the relative abundances of ASV sequences.

Total number of raw reads has been added to the Table S9. Sequence data from this study have been deposited in the European Nucleotide Archive with the primary accession code PRJEB86668.

Spatial analysis

The software 'ArcGIS Pro 3.3.3' was used to analyse and map the temporal and spatial changes of environmental characteristics and soil microbial diversity. Using the *Minimum Bounding Geometry* tool, a polygon for interpolation was created from sample area points. The geometry type was set to envelope. The sample area polygon was extended 5 m outward from the points to visualize the edge effects during interpolation. A 1-m resolution geoTIFF from the Estonian Land and Spatial Development Board (Land and Spatial Development Board 2025) was used for surface elevation data (map sheet 54 693, at a 1:10 000 scale). Elevation values were obtained for each sampling point using the *Extract Values to Points* tool. The surface elevation model was used to create a Local Scene, which displays 3D maps in ArcGIS Pro. A five-fold vertical exaggeration was applied to the terrain to show the area's terrain on the map.

The inverse distance weighted (IDW) interpolation method was used for interpolation. The Spatial Analyst toolset applied the IDW interpolation method, and the power was set to 2. Power is the distance exponent and controls the significance of surrounding points (Esri 2025). Average values for each period were used for interpolating soil emissions, soil moisture, sequencing data (methanotrophy, NO_3^- reduction, and N_2 fixation), and qPCR data (marker gene abundances).

Statistical analyses

The software 'R version 4.3.2' (R Core Team 2023) and 'RStudio 2022.12.0' were used for statistical analysis. Friedman *post hoc* pairwise Wilcoxon test with *pairwise_wilcox_test()* function from the rstatix package (Kassambara 2023a) was used to see which specific pairs of experimental periods (PRE, EXP, POST, and POSTPOST) differed in marker gene abundances. Also, two-sample *t*-tests were conducted to evaluate the effect of flooding on marker gene abundances within each experimental period. Log-transformed abundances were subset by period, and the Welch two-sample *t*-test was applied to compare control and treatment groups. The analysis was performed using the *t.test()* function from the *stats* package in R (R Core Team 2023), and *P*-values below .05 were considered statistically significant.

In addition to that, the Kruskal–Wallis test was used to determine the significant differences between each marker gene abundance in different experimental periods and sample areas. Pairwise comparisons for marker genes with a significant result ($P < .05$) in the Kruskal–Wallis test were conducted using the Wilcoxon rank-sum test. Functions *kruskal.test()* and *pairwise.wilcox.test()* from the *stats* package (R Core Team 2023) was used, and adjusted *P*-values below .05 were considered statistically significant. Benjamini–Hochberg corrected adjusted *P*-values ($P < .05$) were used.

Two-sample *t*-tests were conducted to evaluate the effect of flooding on marker gene abundances within each experimental period. Log-transformed abundances were subset by period, and the Welch two-sample *t*-test was applied to compare control and treatment groups. The analysis was performed using the *t.test()* function from the *stats* package in R (R Core Team 2023), and *P*-values below .05 were considered statistically significant.

The Wilcoxon test was applied to evaluate statistically significant relationships between diversity indices The *stat_compare_means()* function from the ggpubr package (Kassambara 2023b) was used to assess the changes in diversity indices during the experimental period. Significance of changes in bacterial and fungal genera and AMF family relative abundance were tested with the Wilcoxon test wilcox.test() function; Benjamini–Hochberg corrected adjusted *P*-values ($P < .05$) were added with *p.adjust()* function from stats package (R Core Team 2023). The average diversity indices and genera abundance of the PRE and EXP, EXP, and POST, and PRE and POST were compared in both sampling areas (FP and CP).

Multivariate linear models were used to assess soil environmental factors and emissions across different time periods and plots. Model significance was evaluated using 9999 permutations via the *anova()* function from the mvabund package (Wang et al. 2022b). Spearman rank correlation coefficients were used to assess the relationships between environmental factors, diversity, and target gene abundances in the different experimental periods on the FP. The *rcorr()* function from the Hmisc package (Harrell Jr. 2019) was used to calculate the Spearman correlations and the significance ($P < .05$) of the relationship.

The Mantel test was used to show a significant relationship between physico-chemical characteristics, marker gene abundances (qPCR), functional processes and diversity indices (sequencing data) with soil N_2O and CH_4 emissions in the different experimental periods on the FP. Matrices with environmental and emission data mean values were created for each experimental period × sample combination. A point matrix was created from the longitude and latitude data of the sample points. The function *mantel.partial()* from the vegan package (Oksanen et al. 2022) was used for the Mantel statistic representing matrix correlation between three dissimilarity matrices. Spearman correlation method with 999 permutations was used.

Redundancy analysis (RDA) and principal components analysis (PCA) were used to explore relationships between microbial communities (bacteria, fungi, and AMF), environmental variables and soil fluxes. The missMDA package (Josse and Husson 2016), which imputes missing values, was used to fill in the environmental data table for RDA analysis. The function *estim_ncpPCA()* was used to estimate the number of dimensions to use, and the *imputePCA()* function was used to fill in the data gaps with the previously estimated number of dimensions. RDA and PCA plots were created with the *tax_transform()*, *ord_calc()*, and *ord_plot()* functions from the microViz package (Barnett 2024) and 15 most abundant genera were plotted. Microbial taxa relative

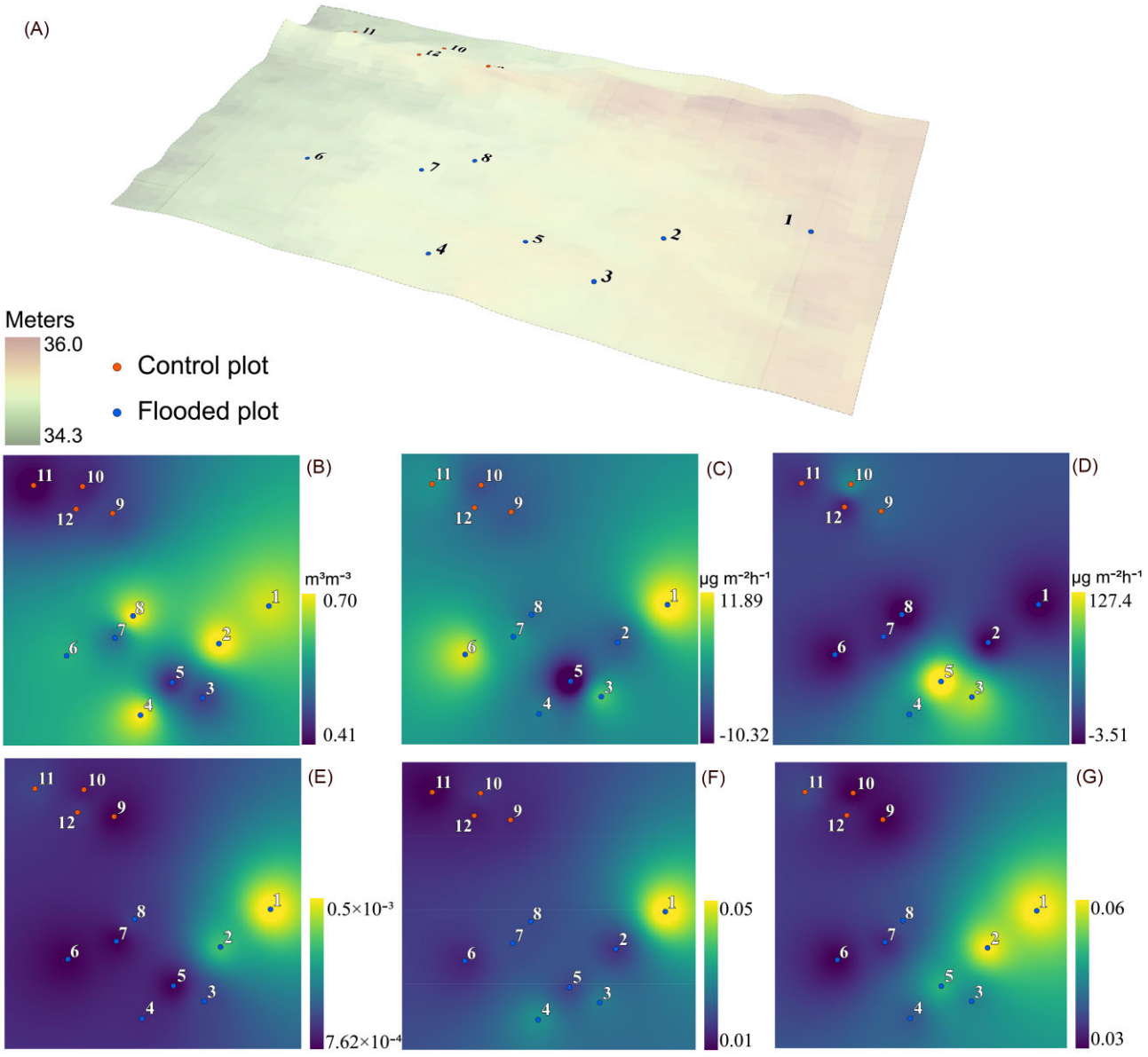

Figure 1. Sampling area elevation (A), soil moisture (B), soil CH_4 fluxes (C), N_2O fluxes (D), methanotrophy (E), NO_3^- reduction (F), and N_2 fixation (G) during the EXP period. CP sampling points (9-12) are shown in red, and FP sampling points (1-8) are shown in blue. The relative abundance of functionally annotated taxa from the sequencing data (FAPROTAX) was used for interpolation (E–G).

abundances were transformed using the centred log-ratio transformation ('clr') prior to applying PCA and RDA. The RDA and PCA microbial data were aggregated with *tax_agg()* function, displayed at the genus level (family level for AMF), and visualized with the ggplot2 package (Wickham 2016). The RDA graphs were divided into three separate plots to enhance readability and clarity. PCA graphs are presented in Fig. S2. Permutation-based multivariate analysis of variance (PERMANOVA) was used to assess the effect of treatment, experiment, and their interaction on the bacterial, fungal, and AMF communities, using the vegan package *adonis2* (Oksanen et al. 2022) with Bray–Curtis dissimilarity and 999 permutations.

Microbial community composition was analyzed using non-metric multidimensional scaling (NMDS) based on Bray–Curtis dissimilarities. Prior to ordination, relative abundance was calculated and low-abundance genera were filtered to retain the 15 most abundant taxa. NMDS was performed using the *ordinate()* and *plot_ordination()* functions from phyloseq package (McMurdie and Holmes 2013). NDMS figures are added to the Supplementary material (Figs S8–S10).

Results

Soil CH_4 and N_2O fluxes

The sampling area elevation range is shown in Fig. 1(A). Soil moisture was higher in the FP during the EXP period than in the CP, but points 3 and 5 in the FP had lower soil moisture than other FP sampling points (Fig. 1B). Flooding had no significant effect on soil N_2O emissions (Schindler et al. 2020), but interpolation results showed that the points with lower soil moisture in the FP (points 3 and 5) had the highest N_2O emissions (Fig. 1D). These points are located at higher elevations than the surrounding area. Soil CH_4 emissions were significantly higher in the FP during the EXP (Schindler et al. 2020). However, the interpolation results indicate that there are points in the FP that act as both CH_4 sinks and sources (Fig. 1C).

Functional annotation of prokaryotic taxa (FAPROTAX) revealed that genetic potential for methanotrophy was highest at points 1 and 2 in the FP (Fig. 1E). The highest proportion of NO_3^- reducers was also observed at point 1 (Fig. 1F). On average, FPs hosted a higher proportion of NO_3^- reducers and N_2 fixers (Fig. 1G).

Bacterial relative abundance and diversity

Based on sequencing data, the bacteria in the study area were classified into 47 phyla and 316 different genera. The most abundant phyla were *Bacteroidota*, *Pseudomonadota*, *Acidobacteriota*, *Verrucomicrobiota*, and *Nitrospirota* (Fig. 2A). The most abundant genera were *Flavobacterium*, *Terrimonas*, *MND1*, Candidatus *Solibacter*, and *Ferruginibacter* (Fig. 2B).

Within study plots, Shannon index (H') of bacteria showed statistically significant differences between the preflood period (PRE) and flooding period (EXP) periods (CP: $P < .001$, FP: $P < .001$) and between the EXP and postflood period (POST) periods (CP: $P < .01$, FP: $P < .001$) in both plots (Fig. 2C), with the index decreasing during the EXP period and increasing again during the POST period. Also, PERMANOVA (Table S6) indicated that the treatment had a small, yet statistically significant effect ($R^2 = 0.059$, $P < .001$) on the bacterial community composition (Fig. S2). Experimental periods also showed a statistically significant effect ($P < .01$) on bacterial community composition ($R^2 = 0.052$). Also, NMDS results showed that the bacterial community in the FP was more variable, with points distributed over a wider area that also encompassed the CP (Fig. S8).

The relative abundance of the genus *Flavobacterium* decreased in both study areas after the EXP period. However, the decrease was significant only in CP ($P < .05$) (Fig. 3A). The relative abundance of *Bradyrhizobium* increased significantly during EXP period ($P < .05$) and decreased in POST period ($P < .05$) in the CP. In contrast, the relative abundance of genus *Gaiella* increased ($P < .01$) after the EXP period in the CP. The relative abundances of *Bradyrhizobium* and *Gaiella* did not change significantly in the FP.

The relative abundance of Candidatus *Omnitrophus* decreased substantially in both study areas (CT $P < .05$; FP $P < .01$). The relative abundance of Candidatus *Udaeobacter* decreased significantly during the EXP period in the CP ($P < .05$), and only significant change in the FP occurred a year later when the relative abundance increased ($P < .05$).

In the FP, the relative abundances of *Geomonas*, *Oleiharenicola*, and *Pelotalea* (Fig. 3B) increased significantly (respectively, $P < .01$, $P < .05$, and $P < .05$) during the flood. The relative abundance of *Solirubrobacter* decreased significantly during the flood ($P < .05$) and increased after the flood ($P < .05$) in the FP. The relative abundance of *Aurantisolimonas* also increased significantly after the flood ($P < .05$) and decreased a year later ($P < .05$). The relative abundance of *GOUTA6* decreased ($P < .05$), while *Paludibaculum* increased significantly ($P < .05$) a year later (POSTPOST period) in the FP.

No significant changes in the relative abundances of *Geomonas*, *Pelotalea*, *Aurantisolimonas*, *GOUTA6*, and *Paludibaculum* were observed in the CP. Additionally, the relative abundances of ammonia-oxidizing bacteria (AOB) from the *MND1* and *Ellin6067* genera (Fig. S3) exhibited changes during the flood; however, the observed increases in abundance were not statistically significant.

Fungal relative abundance and diversity

The proportions of fungal phyla were generally similar between the sampling areas and experimental periods. Based on sequencing data, 34 phyla were identified in the sampling areas, all represented in the FP and 32 in the CP. PCA and (Fig. S2B) NMDS analysis (Fig. S9) revealed overlapping fungal communities in the flooded and CPs, with the dominant genera occurring in both sample area (Fig. S8). Consistently, PERMANOVA (Table S7) and the Shannon index (H'; Fig. 4C) indicated no significant differences in fungal diversity between treatments.

The most abundant fungal phyla were *Basidiobolomycota*, *Mortierellomycota*, *Ascomycota*, *Chytridiomycota*, and *Rozellomycota* (Fig. 4A). 714 fungal genera were identified in the sampling area, with 623 in the FP and 542 in the CP. The most abundant fungal genera in both areas were *Mortierella*, *Hebelomataceae*, and *Naucoria* (Fig. 4B).

During the flood in the FP, the relative abundance of *Rozellomycota* group *GS02* (formerly *Cryptomycota*; Tedersoo et al. 2017a, Kõljalg et al. 2020) and the relative abundance of *Melampsoridium* increased significantly ($P < .01$ and $P < .05$, respectively), while the relative abundance of *Coprinellus* decreased significantly ($P < .05$) (Fig. 5B). The relative abundance of *Cercomonadida* decreased significantly in both sampling areas during the flood (CP $P < .01$ and FP $P < .01$). In the CP, the relative abundances of *Chytridiomycota*, *Limnoperdaceae*, and *Melampsoridium* increased ($P < .01$, $P < .05$, and $P < .01$, respectively), while the relative abundance of *Paxillus* decreased during the flood ($P < .05$).

After the flood, the relative abundance of *Chytridiomycota* decreased significantly in both sampling areas (CP $P <. 01$ and FP $P < .05$). Similarly, in the FP, the relative abundance of *Oliveonia* decreased after the flood ($P < .01$). After the flood, the relative abundance of *Cercomonadida* increased, but the changes were significant only in the FP ($P < .05$). The relative abundance of *Operculomyces* decreased significantly after the flood in the CP ($P < .05$) but not in the FP. A year later, the relative abundances of *Hebelomataceae* and *Amphisphaeriaceae* increased significantly only in the FP ($P < .01$ and $P < .05$, respectively; Fig. 5B).

Opposite to CP, no significant changes were observed for *Limnoperdaceae*, *Paxillus*, and *Chytridiomycota* in FP. The most abundant fungal genera *Mortierella* relative abundance decreased during the flood and increased after the flood (Fig. 4B), but the changes were not statistically significant (Table S5). The proportions of *Mollisia* and *Peziza*, which each constituted <1% of the overall fungal community before the flood and in the CP, but the abundances increased during the flood in the FP and decreased again after the flood (Fig. 4B).

Arbuscular mycorrhizal fungal relative abundance and diversity

In addition to all fungi, we specifically focused on AMF relative abundance, diversity, and their relation to environmental characteristics. Sequencing data revealed that AMF diversity did not change significantly during or after the flood (Fig. 6D), but PERMANOVA (Table S8) showed that treatment and experiment periods had a statistically significant effect (both $P < .001$) on the AMF community (Fig. S2). Treatment explained ~6.9% of the variance ($R^2 = 0.069$), while experiment accounted for about 8.8% ($R^2 = 0.088$). In agreement, NMDS ordination showed partial separation of FP and CP samples, rather than complete overlap (Fig. S10). Furthermore, the patterns in the ITS marker dataset for AMF were similar to those in the AMF marker dataset at the family level (Fig. S11).

At all time points, the AMF family with the highest relative abundance in the CP was *Claroideoglomeraceae* (Fig. 6A). In the

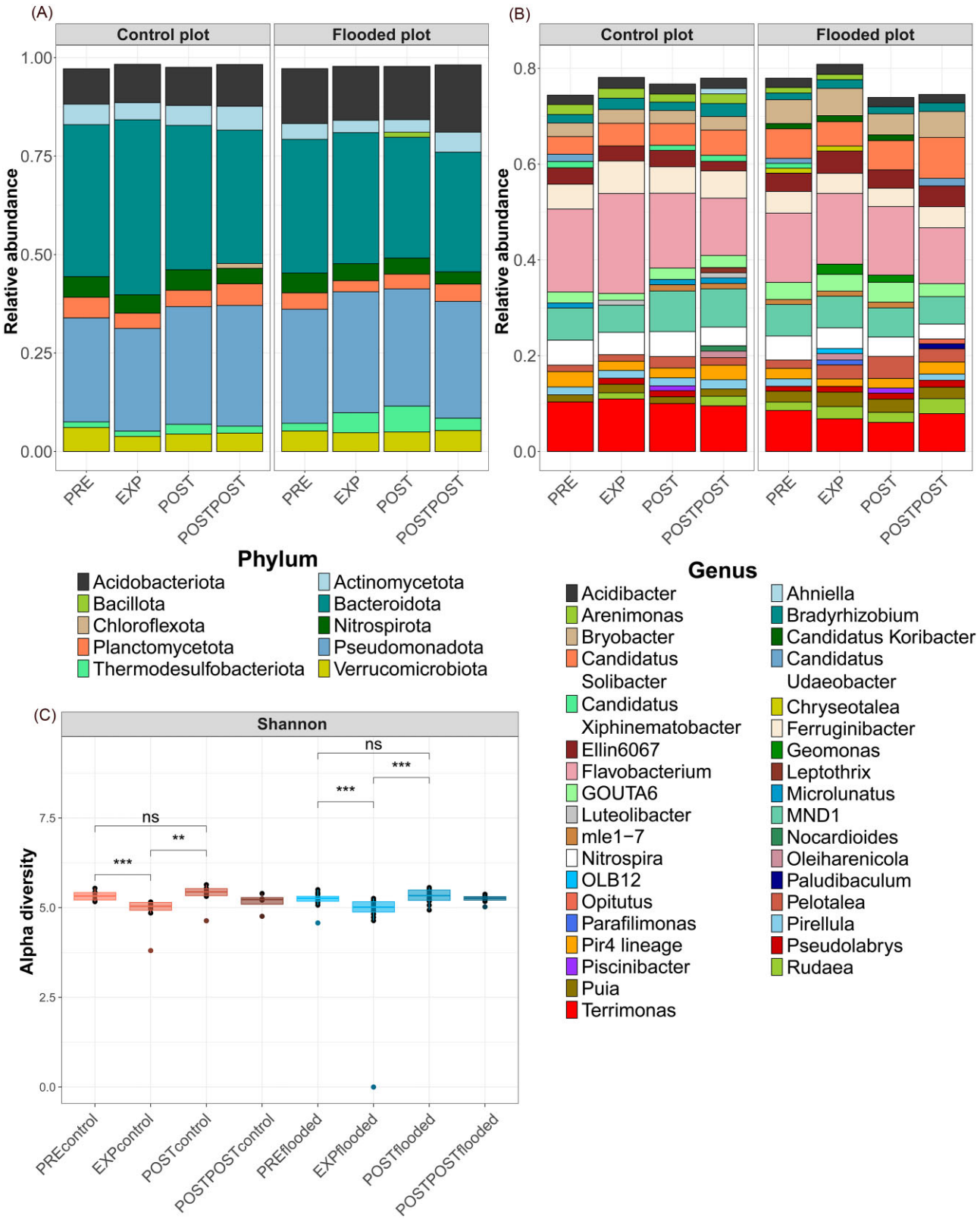

Figure 2. Relative abundances of bacteria at the phylum (A) and genus (B) levels in the CP and the FPs during different experiment periods in the riparian *A. incana* forest. Taxonomic classification of sequencing data was performed using the SILVA v138.2 database (Quast et al. 2013). Panel C shows changes in the bacterial Shannon index during the experiment. Red bars represent CP and blue bars represent FP. The asterisk (*) indicates a statistically significant difference between the experiment periods ($P < .05$ = '*', $P < .01$ = '**', and $P < .001$ = '***'). The flooding consisted of a 14-day continuous soil inundation during the growing season. Abbreviations: preflood period (PRE), flooding period (EXP), postflood period (POST), and a year after the flooding (POSTPOST).

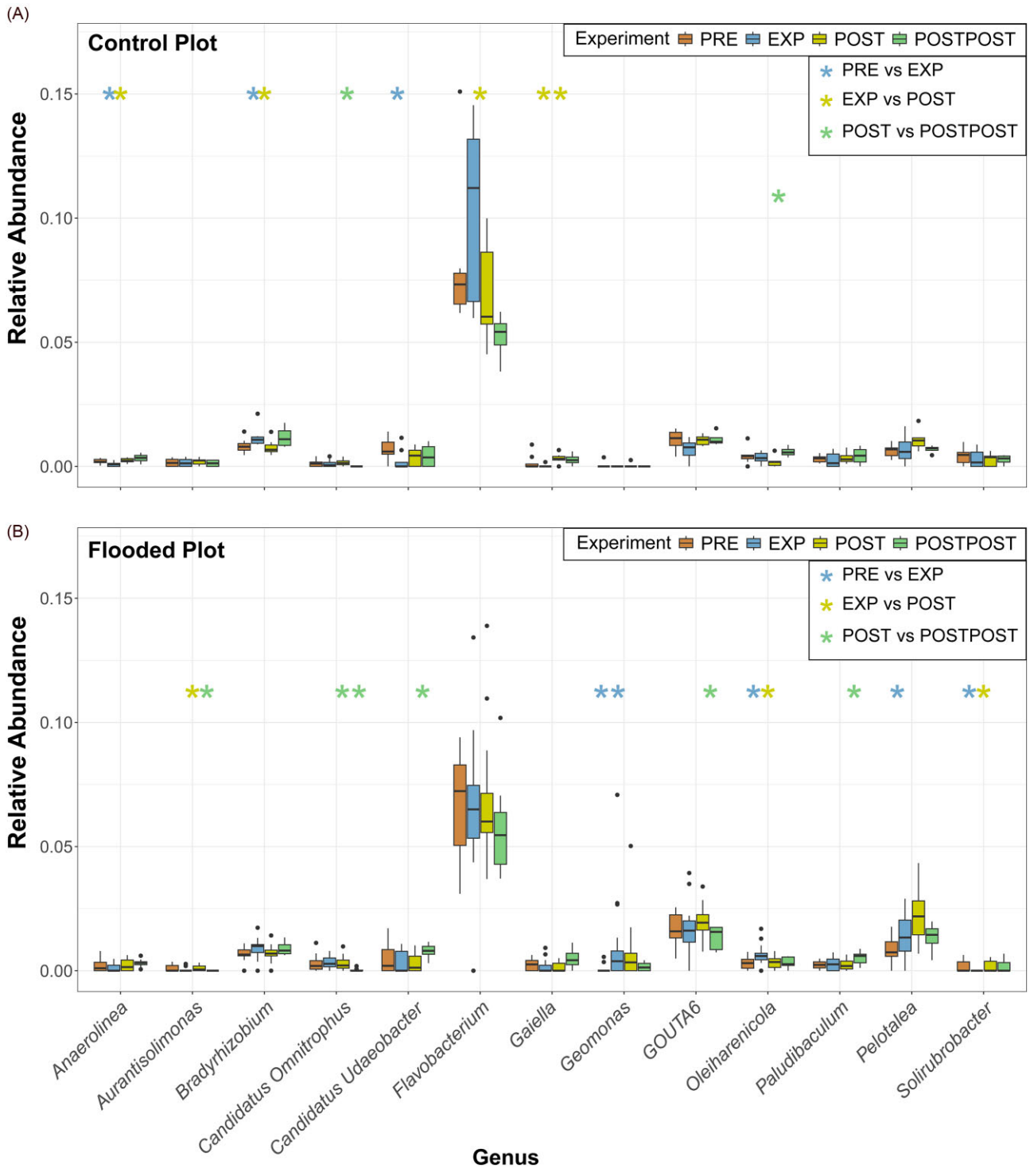

Figure 3. Changes in the relative abundance of bacterial genera in the CP (A) and FP (B), based on sequencing data. The Wilcoxon rank-sum test determined statistically significant differences between periods (PRE vs. EXP, EXP vs. POST, and POST vs. POSTPOST). Asterisks (∗) indicate statistical significance (∗—$P < .05$, ∗∗—$P < .01$, and ∗∗∗—$P < .001$), with blue, yellow, and green denoting changes between PRE-EXP, EXP-POST, and POST-POSTPOST, respectively. Abbreviations: preflood period (PRE), flooding period (EXP), postflood period (POST), and a year after the flooding (POSTPOST).

FP, the dominant family shifted during the experiment, with *Archaeosporaceae* showing the highest relative abundance before the flood and *Acaulosporaceae* and *Claroideoglomeraceae* showing high relative abundances at other times (Fig. 6A). Experimental flooding increased the relative abundance of *Acaulosporaceae* in the FP, but there were no changes in CP ($P < .05$; Fig. 6B and C). After the flood, the relative abundance of the *Acaulosporaceae* decreased ($P < .05$) and *Claroideoglomeraceae* (not significantly) in FP. A year after the flooding (POSTPOST), the relative abundance of *Claroideoglomeraceae* in the FP increased ($P < .05$). There were no significant changes in the relative abundances of AMF families in CP during the experiment phases.

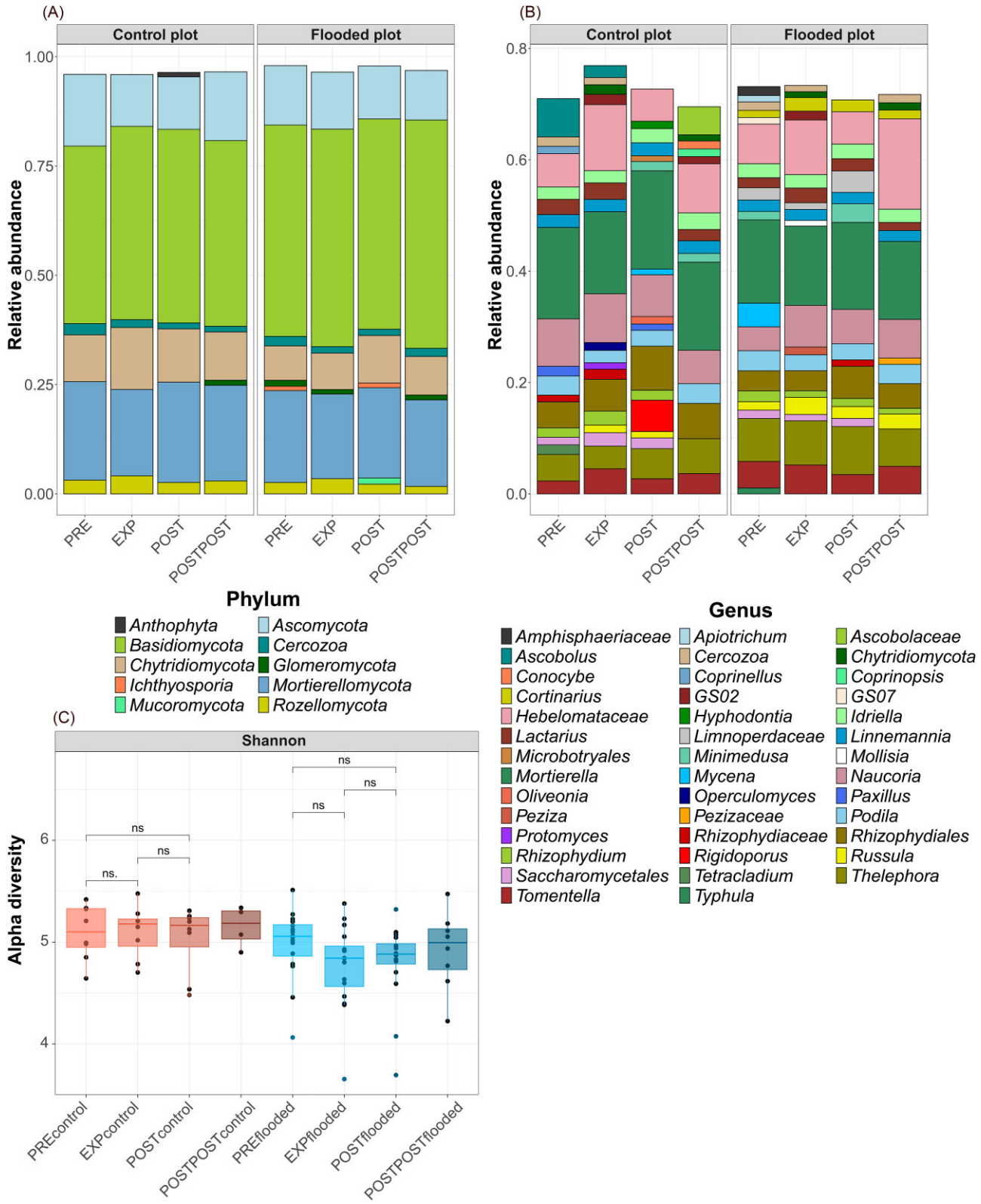

Figure 4. Relative abundances of fungi at the phylum (A) and genus (or family) (B) levels in the CPs and the FPs during different experiment periods, based on sequencing data. Panel C shows changes in the fungal Shannon diversity index during the experiment. Red bars represent CP, and blue bars represent FP. The asterisk (∗) indicates a statistically significant difference between the experiment periods ($P < .05$ = '∗', $P < .01$ = '∗∗', and $P < .001$ = '∗∗∗'). Abbreviations: preflood period (PRE), flooding period (EXP), postflood period (POST), and a year after the flooding (POSTPOST).

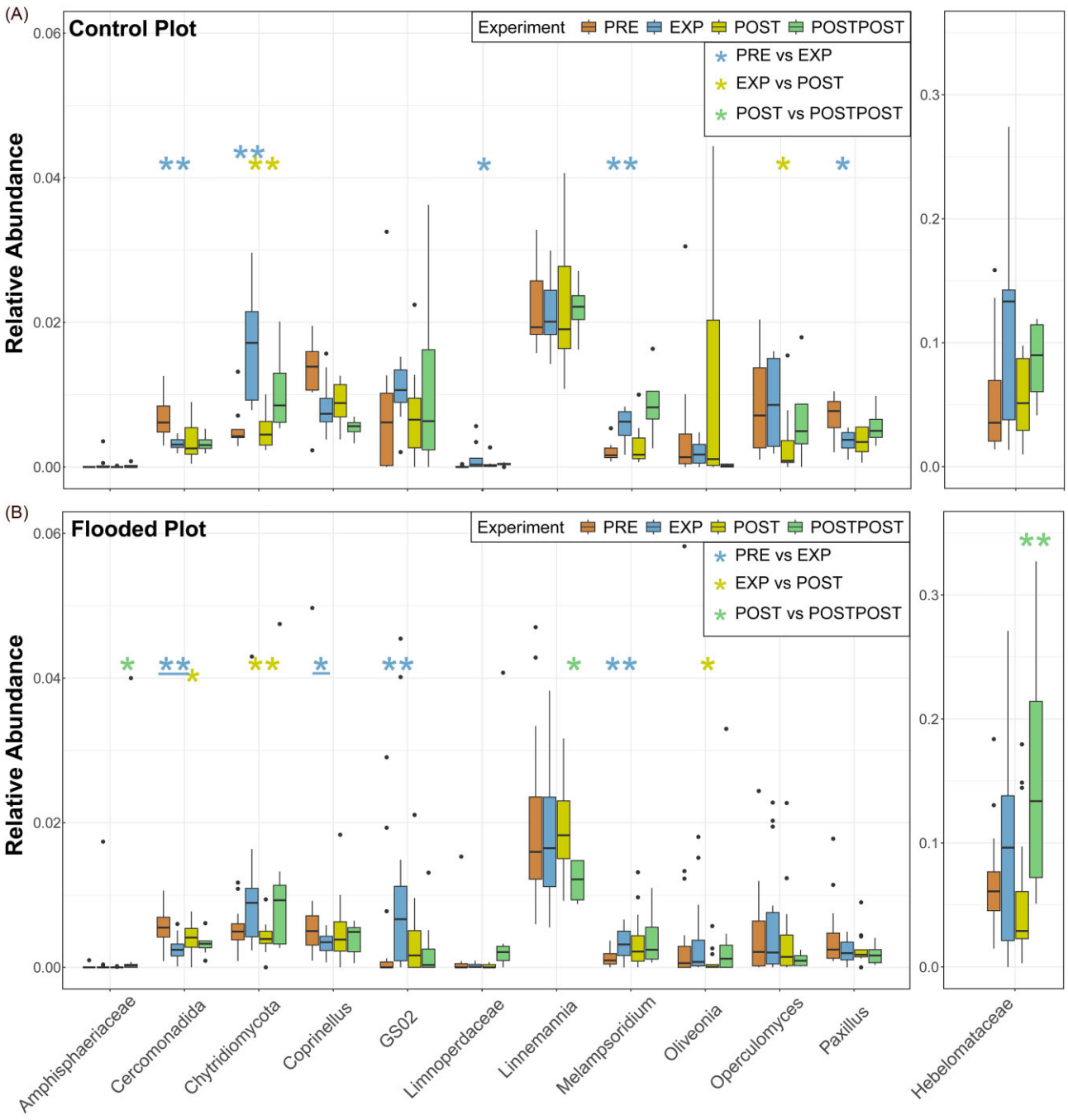

Figure 5. Significant changes in fungal genus relative abundances in the CP (A) and FP (B), based on sequencing data. The Wilcoxon rank-sum test determined statistically significant differences between periods (PRE vs. EXP, EXP vs. POST, and POST vs. POSTPOST). Asterisks (∗) indicate statistical significance (∗—$P < .05$, ∗∗—$P < .01$, and ∗∗∗—$P < .001$), with blue, yellow, and green denoting changes between PRE-EXP, EXP-POST, and POST-POSTPOST, respectively. Line under the asterisks indicates Benjamini–Hochberg corrected ($P < .05$) Wilcoxon rank-sum test. Abbreviations: preflood period (PRE), flooding period (EXP), postflood period (POST), and a year after the flooding (POSTPOST).

Abundances of functional genes of the microbial nitrogen and methane cycles

The significant changes in marker gene abundances between the sample areas are shown in Table S2, and changes between the experiment periods are shown in Tables S3 and S4. qPCR results showed, that archaeal *amoA* gene copy numbers were statistically lower in the FP than in CP ($P < .05$) throughout the experimental period (Fig. 7A). Flooding had a significant effect on archaeal *amoA* as the abundance decreased during the flood and increased after the flooding ($P < .05$). Bacterial *amoA* abundances significantly differed between the sampling plots before the flood ($P < .05$), but these differences disappeared after the flood (Fig. 7B). In the CP, changes in bacterial *amoA* abundance were not significant. In the FP, COMAMMOX *amoA* gene copy numbers decreased during and after the flood (Fig. 7C), and abundance before the flood differed significantly from the EXP and POST periods ($P < .05$). A year later (POSTPOST), the COMAMMOX *amoA* gene copy numbers had increased significantly in the FP ($P < .05$). The archaeal communities

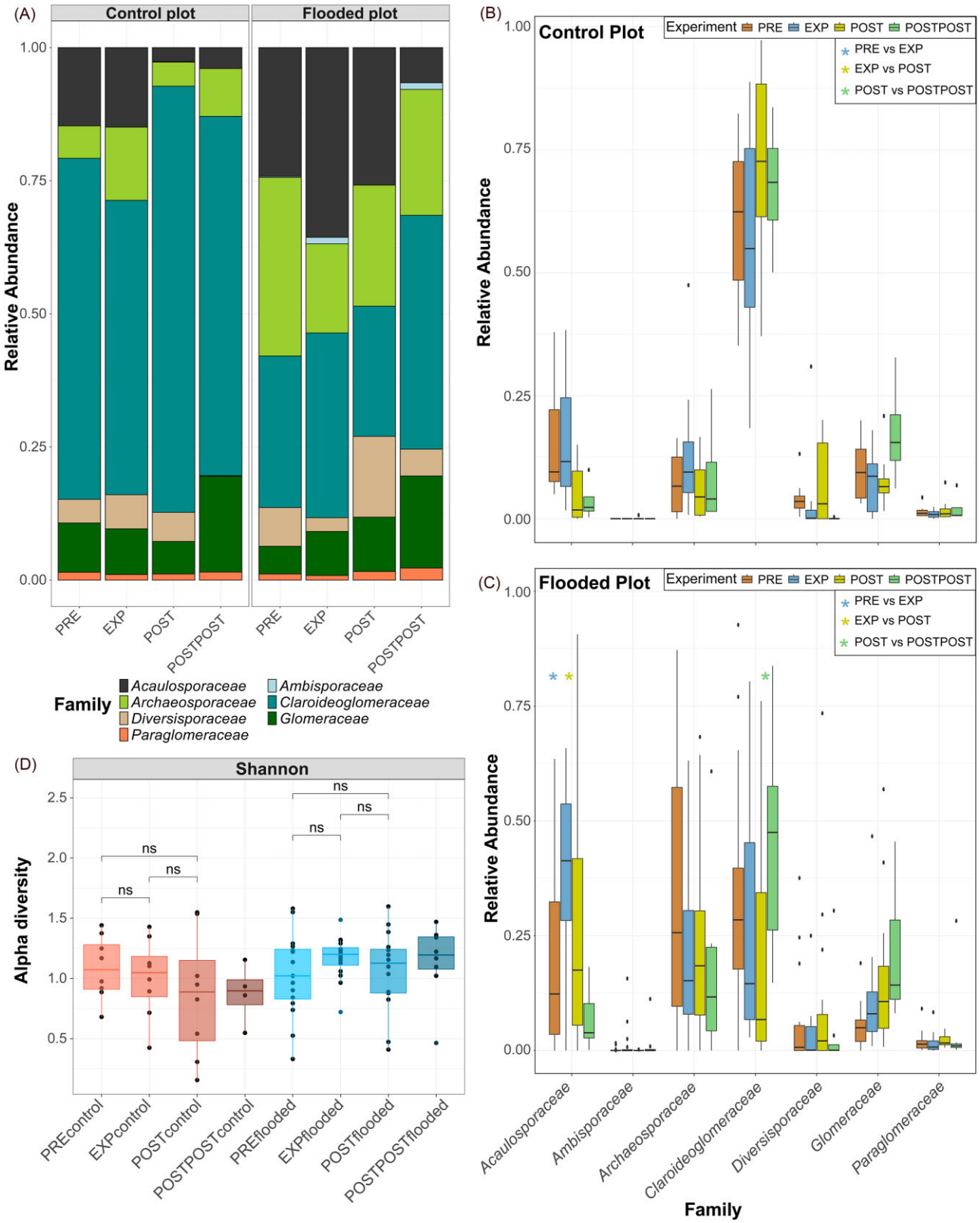

Figure 6. Relative abundances of AMF at the family (A) level in the CPs and FPs during different experiment periods, based on sequencing data. AMF families' relative abundances in the CP (B) and FP (C) at different periods of the experiment. Panel D shows changes in the AMF Shannon diversity index during the experiment. Red bars represent CP, and blue bars represent FP. The Wilcoxon rank-sum test determined statistically significant differences between periods (PRE vs. EXP, EXP vs. POST, and POST vs. POSTPOST). Asterisks (*) indicate statistical significance (*—$P < .05$, **—$P < .01$, and ***—$P < .001$), with blue, yellow, and green denoting changes between PRE-EXP, EXP-POST, and POST-POSTPOST, respectively. Abbreviations: preflood period (PRE), flooding period (EXP), postflood period (POST), and a year after the flooding (POSTPOST).

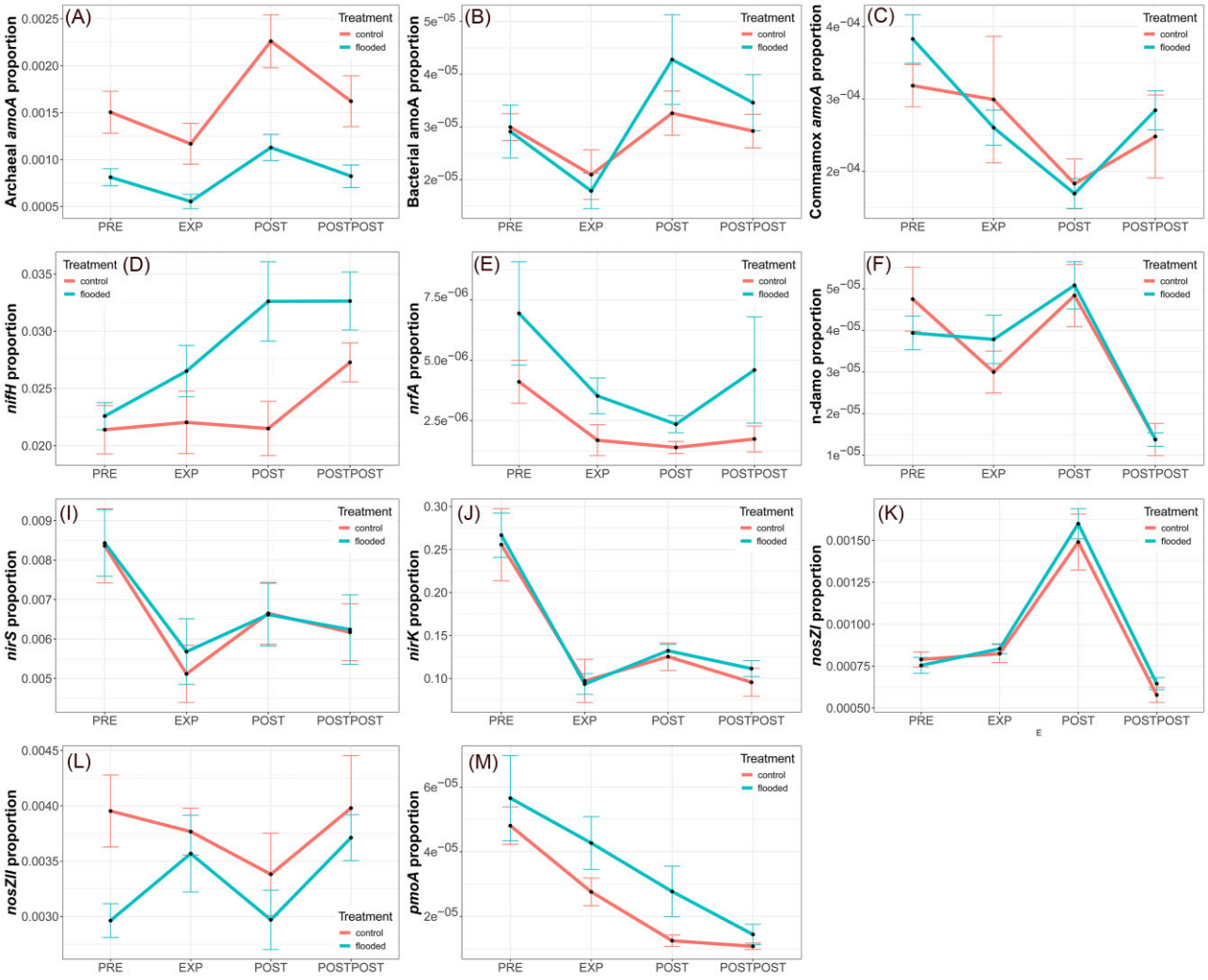

Figure 7. Changes of functional gene proportions in the CP and FP during different experiment periods, based on qPCR. Panels show archeal *amoA* (A), bacterial *amoA* (B), comammox *amoA* (C), *nifH* (D), *nrfA* (E), n-damo (F), *nirS* (I), *nirK* (J), *nosZI* (K), *nosZII* (L), and *pmoA* (M) functional gene proportions. Red lines show the changed of abundance proportion in the CP and blue in the FP. Black points on the line show the mean proportional abundance and errorbars the standard error of the mean. Abbreviations: preflood period (PRE), flooding period (EXP), postflood period (POST), and a year after the flooding (POSTPOST).

were characterized only by the abundance of archaeal 16S rRNA, archaeal *amoA*, and archaeal *mcrA* genes, and no archaeal community sequencing was performed.

Attempts to quantify the *mcrA* gene yielded no detectable amplification, indicating that the gene was either not present or occurred at levels below the detection limit. The abundance of *pmoA* gene copy numbers did not differ between the sample areas before the flooding (Fig. 7M). The flooding significantly affected *pmoA* abundance, with levels significantly higher in the FP than in the CP ($P < .05$).

The abundance of n-damo-specific 16S rRNA gene copy numbers was statistically lower a year after the flood (POSTPOST) (Fig. 7F). The POSTPOST period abundance of the n-damo-specific 16S rRNA genes was different from the PRE, EXP, and POST periods in the FP ($P < .05$). There were no statistically significant changes in n-damo-specific 16S rRNA gene abundances in the CP. *nifH* abundance changes in the FP were not significant, but *nifH* abundance increased with the flooding (Fig. 7D). The only significant changes in the FP were a year later, when the *nifH* abundance was statistically higher than the preflooding abundance and POST period ($P < .05$). The abundance of *nrfA* gene copies was significantly lower after the flood compared to preflood abundances in FP ($P < .05$) (Fig. 7E).

The abundance of *nirK* before the flood was statistically different from EXP, POST, and POSTPOST periods in FP ($P < .05$) (Fig. 7J). Similarly to the abundance of n-damo genes, flooding significantly affected fungal *nirK* gene copy numbers a year later. Fungal *nirK* abundance a year later was significantly higher than in the PRE, EXP, and POST periods at the FP ($P < .05$). There were no statistically significant changes in fungal *nirK* abundances in the CP. The abundance of nirS decreased significantly during the flood in FP ($P < .05$) and PRE period abundance was significantly lower from POST period ($P < .05$) (Fig. 7I). After the flood, the abundance of *nosZI* gene copies increased, and this change in abundance was significantly greater than PRE, EXP, or POSTPOST periods in the FP ($P < .05$) (Fig. 7K). The abundance of *nosZII* gene copies in the CP and the FP differed significantly before the flood ($P < .05$) (Fig. 7L). Statistically significant differences between the areas disappeared during the flood when *nosZII* abundance increased with the flood (not significantly). The abundance on *nosZII* decreased

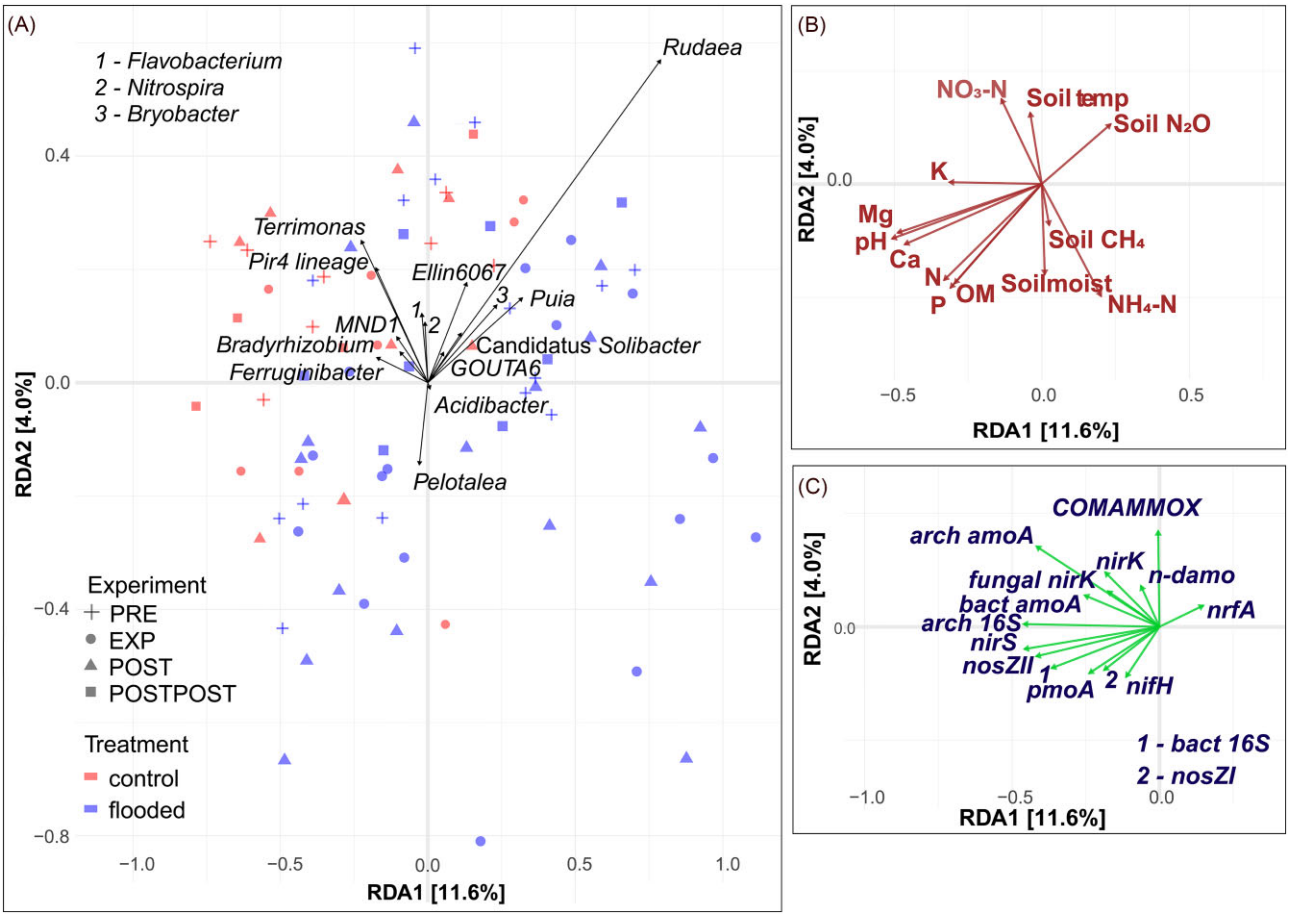

Figure 8. RDA ordination plots showing relationships of bacterial genera relative abundances (A) with soil physico-chemical properties (B), based on sequencing data and marker gene abundances (C), based on qPCR. The RDA was fitted for all variables together, and the biplots were separated into panels (A–C) later for readability. Abbreviations: nitrogen (N), phosphorus (P), soil organic matter (OM), ammonium (NH_4-N), nitrate (NO_3-N), soil methane emission (soil CH_4), soil nitrous oxide emission (soil N_2O), soil temperature (soil temp), potassium (K), magnesium (Mg), calcium (Ca), preflood period (PRE), flooding period (EXP), postflood period (POST), and a year after the flooding (POSTPOST).

significantly after the flood ($P < .05$) and POST period abundance was significantly different ($P < .05$) form PRE on FP. The abundance of *nosZII* gene copy numbers increased significantly a year later at the FP ($P < .05$).

Relationships between taxa, functional gene abundances, environmental characteristics, and GHG fluxes

Sequencing results suggested that bacterial genera *Terrimonas*, *Pir4 lineage*, *Nitrospira*, *Ellin6067*, and *MND1* were relatively more abundant in areas with higher soil NO_3^- concentrations. From Fig. 8(B) and (C), the genera were positively related also with nitrification COMAMMOX *amoA*, *nirK* abundance, and soil temperature. On the other hand, *Acidibacter* was more abundant in areas with lower NO_3^- concentrations and higher NH_4^+ concentrations (Fig. 8A and B). *Rudaea*, *Byrobacter*, *Puia*, *GOUTA6*, Candidatus *Solibacter*, *Ellin6067*, and *Nitrospira* in were more abundant in drier areas were positively related to soil N_2O emissions (Fig. 8A and B). Abundances of the bacterial genera *Acidibacter* and *Pelotalea* were positively related to soil CH_4 fluxes and soil moisture (Fig. 8A and B).

Fungal taxonomic groups *Tomentella* and *Hebelomataceae* were relatively more abundant in areas with higher soil NH_4^+ concentrations and positively related to soil N_2O emission and soil moisture. *Tomentella* and *Hebelomatacea* were less abundant in areas with lower NO_3^- and K concentrations. In contrast, *Ascobolus* and *Rhizophydiales* were more abundant in the opposite environment (Fig. 9A and B).

Fungal relative abundances of *Saccharomycetales*, *Podila*, *Idriella*, and *Limnoperdaceae* were positively correlated with soil Mg, Ca, and pH. Relative abundances of *Linnemannia*, *Rhizophydium*, and *Lactarius* more abundant in areas with soil CH_4 emissions but RDA also showed that the genera were negatively associated with soil moisture (Fig. 9A and B). Among the analysed fungal genera, the genus *Russula* was most closely and positively associated with soil N_2O emissions, and the fungal taxonomic group was also more abundant in soils with higher soil NH_4^+ concentrations (Fig. 9A and B).

AMF family *Diversisporaceae* was positively correlated with soil NO_3^- concentration and temperature (Fig. 10A and B). *Archaeosporaceae* and *Ambisporaceae* were negatively related to soil NO_3^- concentration and temperature, and positively related to Ca, Mg, N, OM, and P. Also, the relative abundance of *Archaeosporaceae* and *Ambisporaceae* were positively related to soil moisture and CH_4 emissions. *Claroideoglomeraceae* were relatively more abundant in environments with higher soil K concentration. In contrast, *Paraglomeraceae* were more abundant in areas with higher pH. Among all the analysed AMF families, *Acaulosporaceae* and *Diversisporaceae* abundances were most closely associated with higher soil N_2O emissions (Fig. 10A and B).

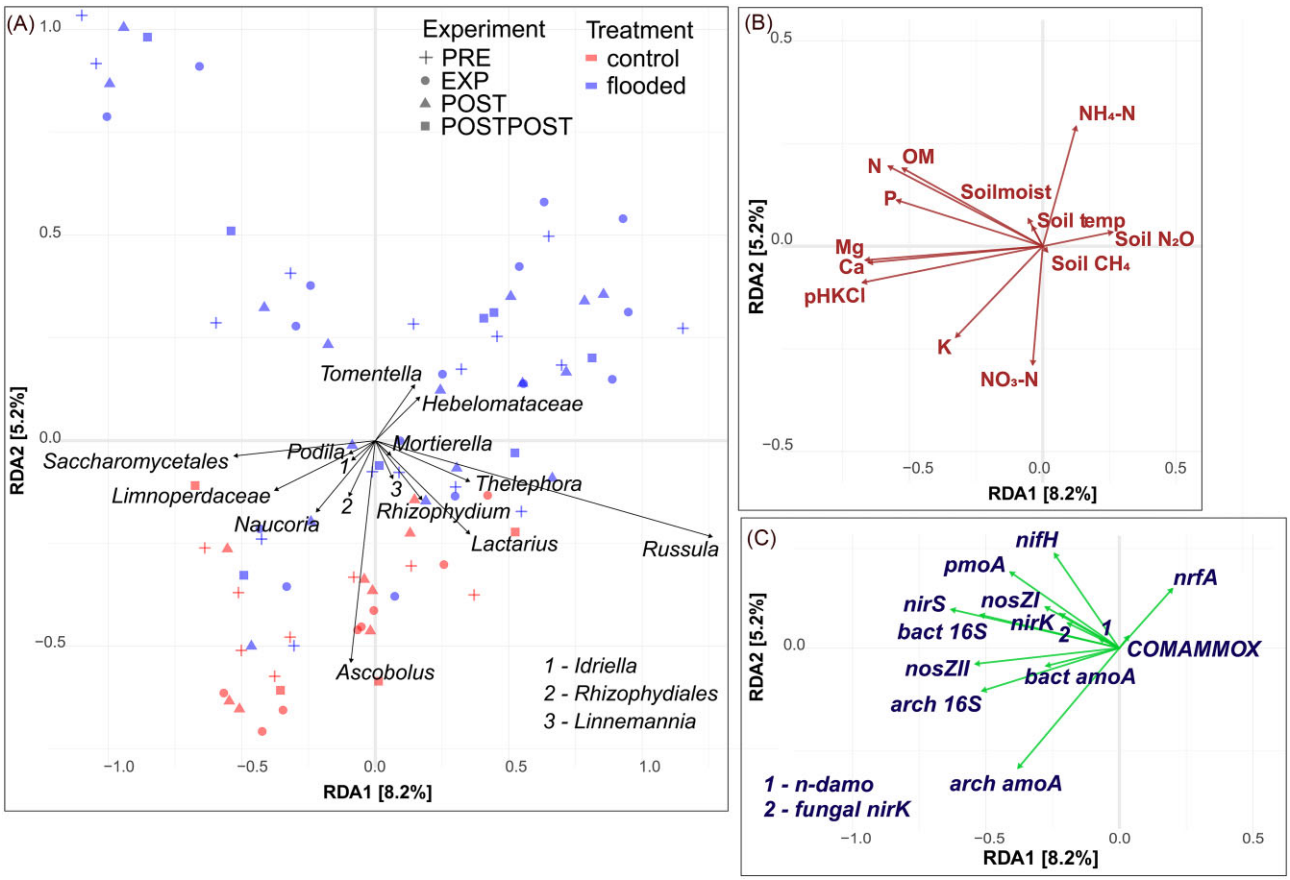

Figure 9. RDA ordination plots showing relationships of fungal genera relative abundances (A) with physico-chemical soil properties (B), based on sequencing data and marker gene abundances (C), based on qPCR. The RDA was fitted for all variables together, and the biplots were separated into panels (A–C) later for readability. Abbreviations: nitrogen (N), phosphorus (P), soil organic matter (OM), ammonium (NH_4-N), nitrate (NO_3-N), soil methane emission (soil CH_4), soil nitrous oxide emission (soil N_2O), soil temperature (soil temp), potassium (K), magnesium (Mg), calcium (Ca), preflood period (PRE), flooding period (EXP), postflood period (POST), and a year after the flooding (POSTPOST).

Correlations between environmental characteristics, functional processes, microbial diversity, and GHG fluxes in the FPs

Correlation analysis showed that fungal diversity and soil K concentration were negatively correlated before the experimental flooding in FP (Fig. S4). During the flooding, bacterial diversity was positively correlated with temperature (Fig. 11). After the flooding, AMF diversity was positively correlated with soil NO_3^- concentration (Fig. S5).

Soil moisture was positively correlated with the abundance of *pmoA* genes before the flooding (Fig. S4) and with bacterial *amoA* and *nosZI* abundances during the flooding in FP (Fig. 11). After the flooding, soil moisture was positively related to the abundance of bacterial *amoA*, *nosZII*, and bacterial 16S rRNA gene (Fig. S5). Additionally, soil moisture was negatively associated with soil NO_3^- concentration but positively with NH_4^+ concentration after the flood in FP.

Mantel test results indicated that soil N_2O emissions were negatively associated with bacterial 16S rRNA gene, bacterial *amoA*, *nirK*, *nirS*, and *nosZII* abundances before the flooding experiment (Fig. S4). During the flood, soil N_2O emissions were negatively correlated with abundances of archaeal 16S rRNA and archaea *amoA* genes but positively with n-damo 16S rRNA gene abundance (Fig. 11). After the flooding, the negative correlations with archaeal abundance persisted, and N_2O emissions were also negatively related to *nosZII* abundance (Fig. S5). Like RDA results, soil N_2O emissions were negatively related to soil moisture during the flood (Fig. 10). Soil CH_4 emissions were positively correlated with Ca during the flood (Fig. 11) and negatively correlated with *nifH* abundance after the flood (Fig. S5).

The processes showed that N_2 fixation was negatively correlated with bacterial diversity during the flood but positively related with *nosZI* abundance after the flood. NO_3^- reduction was negatively correlated with the archaeal 16S rRNA gene and *nosZII* abundance during the flood. Methanotrophy was positively correlated with soil N, Mg, and OM concentrations in the FP during the flood. After the flood, NO_3^- reduction was negatively correlated with the abundance of *nirS*, *nosZII*, and fungal *nirK* genes but positively correlated with *nrfA* abundance (Fig. S5).

Discussion

Temporal changes in microbial diversity in response to flooding

Soil microbial communities in this study varied spatially and temporally in response to environmental characteristics. Floods and soil water content affect microbial communities and GHG emissions in riparian ecosystems (Schindler et al. 2020). Shen et al. (2021) observed lower soil bacterial α-diversity during flooding compared to drought. Similarly, we found that bacterial α-diversity was lower during the flood than before in both sample areas, with heavy rainfall at the end of the flooding experiment po-

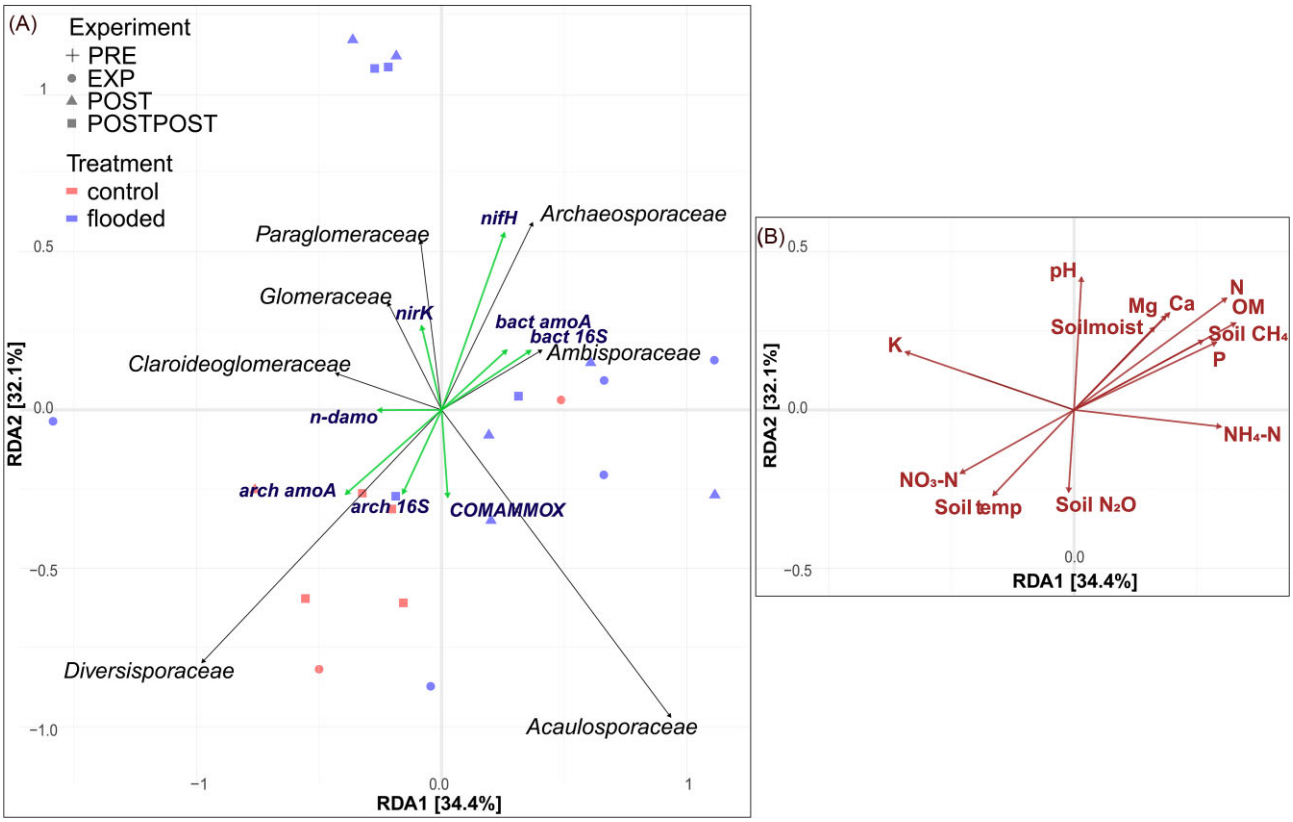

Figure 10. RDA ordination plots showing relationships of AMF families relative abundances (black lines), based on sequencing data with marker gene abundances (green lines), based on qPCR (A) and physico-chemical soil properties (B). The RDA was fitted for all variables together, and the biplots were separated into panels (A–C) later for readability. Abbreviations: nitrogen (N), phosphorus (P), soil organic matter (OM), ammonium (NH_4-N), nitrate (NO_3-N), soil methane emission (soil CH_4), soil nitrous oxide emission (soil N_2O), soil temperature (soil temp), potassium (K), magnesium (Mg), calcium (Ca), preflood period (PRE), flooding period (EXP), postflood period (POST), and a year after the flooding (POSTPOST).

tentially influencing bacterial diversity in the CP. After the flooding event, the bacterial diversity recovered. Drainage and soil water content influence fungal community structure (Schimel et al. 1999, Graça et al. 2021), but fungi have been found to be more resistant to short-term flooding than bacteria (Wang et al. 2022a). Our results showed no significant fungal community changes during or after flooding. As in Unger et al. (2009), we assume that the flooding duration was insufficient to impact the fungal community significantly. Flood duration can be crucial for AMF diversity, with intensive flooding shown to have a negative impact and moderate flooding a positive one (Wang et al. 2011). AMF are aerobic microorganisms (Miller 2000) and AMF spores might not germinate under intensive or prolonged flooded conditions, which can slow down or stop the growth of AMF (Wang et al. 2011). We observed a slight but nonsignificant AMF diversity change under moderate flooding (Fig. 6D). In the case of vegetation, the flooding period may result in some herbaceous layer dieback and vigorous formation of adventitious roots in alder trees (Gill 1975, Ghanbary et al. 2012). The formation of adventitious roots is a classic response to soil anoxic conditions (McDonald et al. 2002).

Spatial variation of microbial communities and nitrogen–carbon cycle genes

At our study site, soil moisture ranged between 0.4 and 0.7 m^3/m^3 (except POSTPOST period), while levels of 0.5–0.6 m^3/m^3 are the largest N_2O source due to favourable conditions for N_2O-forming processes, such as nitrification and denitrification (Bahram et al. 2022). Interpolation results showed that the soil was a source of N_2O during the flood, particularly at drier points within the FP (points 3 and 5), which were slightly elevated. Topography influences N_2O emissions by affecting soil hydrology (Fang et al. 2009, Vilain et al. 2010). At the water content levels of the drier FP points (0.4–0.5 m^3/m^3 water content), N_2O production has been usually linked to nitrification (Congreves et al. 2019). Additionally, there was a negative correlation between N_2O emissions and soil water content during the flood.

The relationship between soil water content and *pmoA* abundance may vary with environmental conditions, but similarly to Yang et al. (2024), we found no correlation between soil water content and *pmoA* abundance (determined by qPCR). Interpolation showed that the relative abundance of methanotrophic 16S rRNA taxa (FAPROTAX) was highest during the flood at points closest to the pumped water, which mimicked intensive rainfall and generated overland runoff. Before the flood, *pmoA* abundances did not differ significantly between CP and FP, but during the flood, abundance was significantly higher at the FP, indicating that pulsed flooding (water was pumped only during the day) affects *pmoA* abundance. Pulsed flooding supports CH_4 oxidation in the topsoil (10 cm) more than continuous flooding (Chowdhury and Dick 2013). Additionally, methanotrophs can oxidize CH_4 even under anaerobic conditions (Caldwell et al. 2008). Anaerobic CH_4 oxidation can couple with different types of electron acceptors, like sulphate (Antler et al. 2014), iron (Oni and Friedrich 2017), nitrate, or nitrite (Zhang et al. 2021b).

We attempted to quantify the *mcrA* gene (qPCR), but no amplification was detected in the samples, indicating that the gene

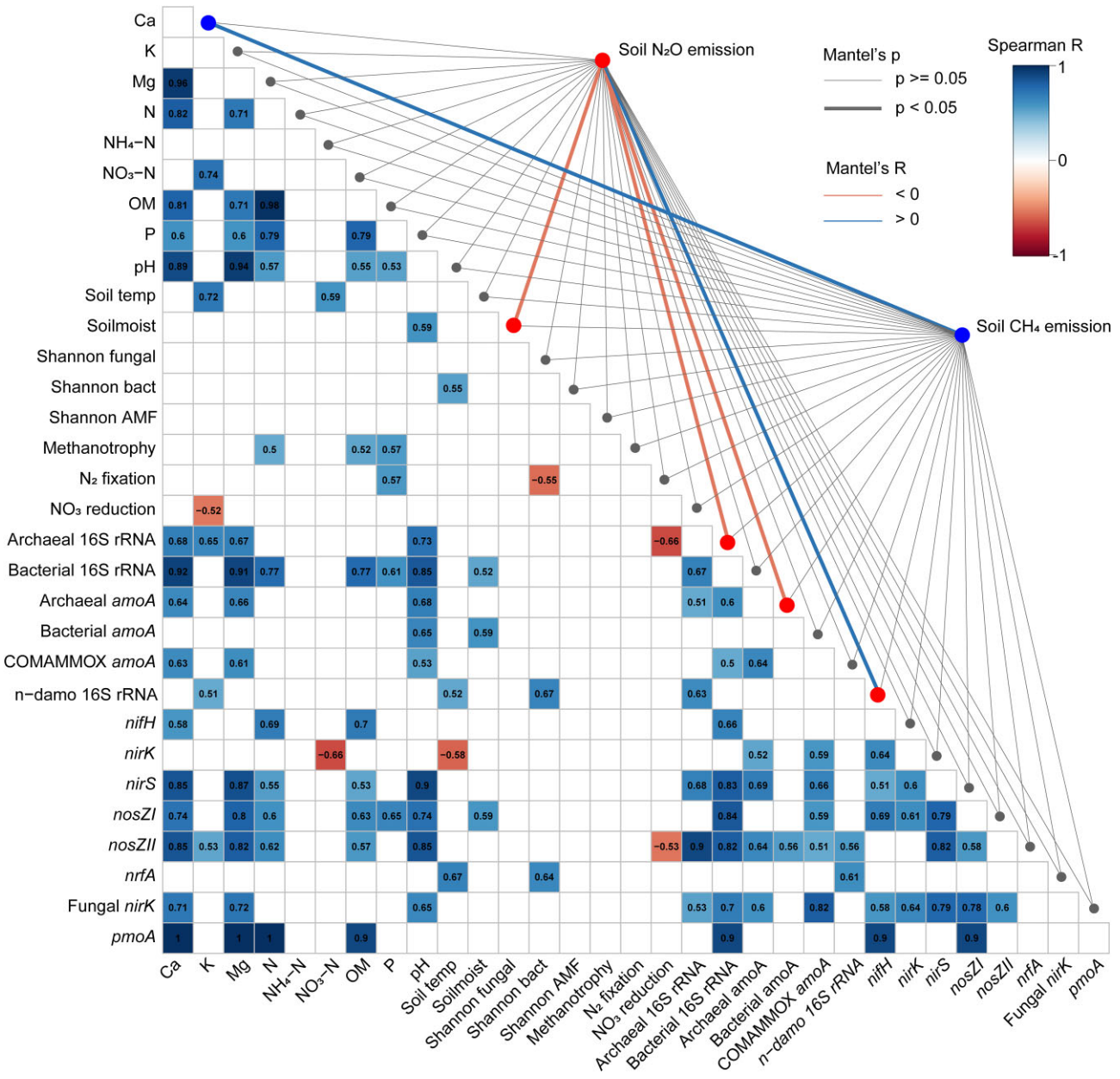

Figure 11. Spearman correlations and Mantel test during the FP flooding (EXP) period. The correlation table displays only significant ($P < .05$) correlations between environmental variables, marker genes, processes, and diversity. Mantel test results show soil N_2O (red endpoints) and CH_4 (blue endpoints) emissions in relation to environmental variables, functional genes (abundances determined with qPCR), processes (based on FAPROTAX), and diversity (based on sequencing data), represented by lines from y-axis. Thick lines indicate significant relationships ($P < .05$), with colour denoting positive (blue line) or negative (red line) relationships.

was either absent or present below the detection limit. Since methanogens are anaerobic, they are likely more abundant in deeper layers, or alternatively, the pulsed flooding or the duration of the flooding period may not have been long enough to create conditions favourable for the presence of the *mcrA* gene.

Temporal shifts in the bacterial communities related to nitrogen and carbon cycling

During the flooding period, soil water content increased significantly in the experimental plot (FP) (Schindler et al. 2020), leading to a shift in the bacterial community with a rise in anaerobic bacteria (Fig. 12). Sequencing data showed that flooding positively affected the strictly anaerobic genera *Pelotalea* and *Geomonas* (Itoh et al. 2021, Xu et al. 2021), which thrive in high-moisture habitats. These iron-reducing bacteria (Itoh et al. 2021, Xu et al. 2021) are linked to dissimilatory iron reduction coupled with organic C oxidation (Canfield et al. 1993, Zhao et al. 2024). Additionally, *Geomonas* is mainly found in paddy soils (Xu et al. 2019, Zhang et al. 2023), and some species can fix N (Xu et al. 2021).

Sequencing results showed that flooding significantly affected the aerobic microorganisms *Solirubrobacter* and *Aurantisolimonas* (Singleton et al. 2003, Liu et al. 2018). The relative abundance of *Solirubrobacter* decreased during the flooding, and it is typically found in extreme environments like deserts (Jiang et al. 2023) but also in agricultural soils (Singleton et al. 2003). The

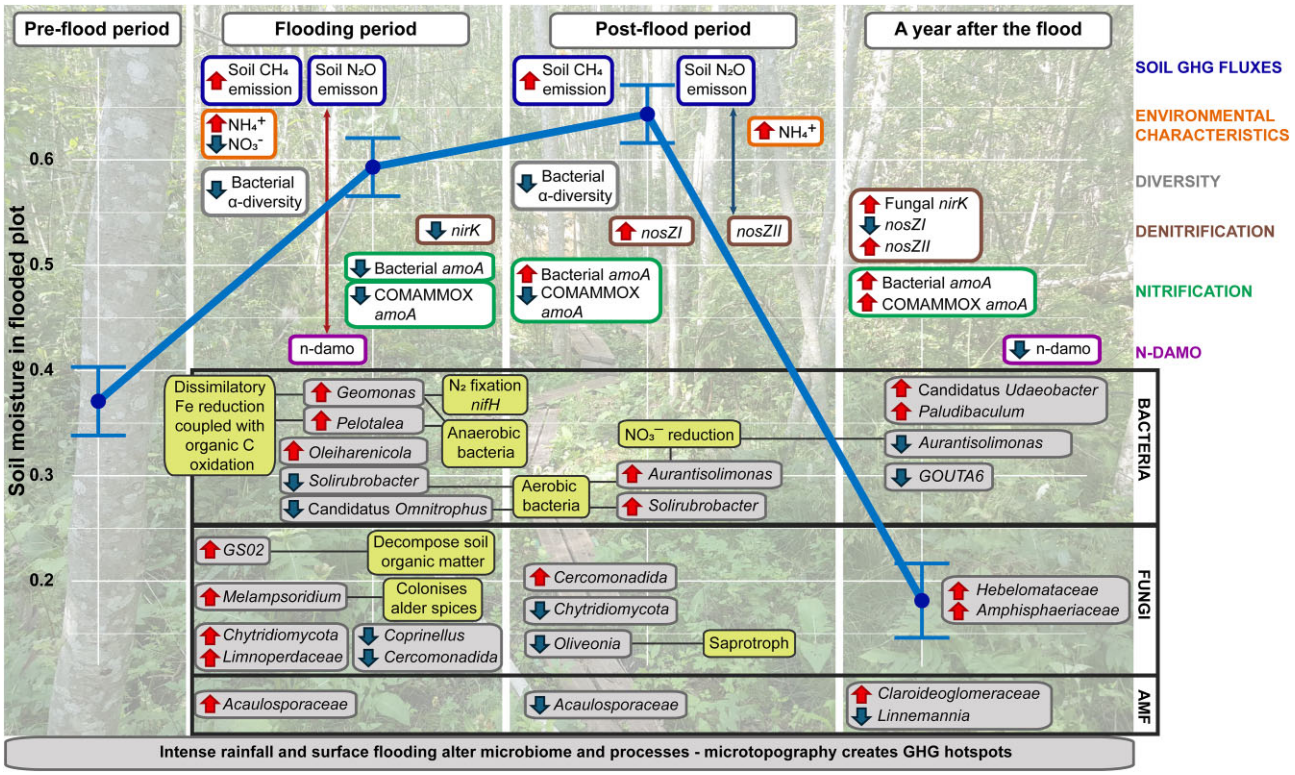

Figure 12. Main changes in the FP observed during the experiment (EXP), after the flood (POST), and 1-year postflood (POSTPOST). The blue line represents soil moisture. Red arrows indicate significant increases, while blue arrows indicate significant decreases ($P < .05$). Lines with two arrow ends show significant correlations ($P < .05$), red positive and blue negative correlation. Black lines highlight potential chemical or ecological traits of the genera that are shown in yellow boxes.

relative abundance of *Aurantisolimonas* increased after the flood. In this genus, a single species, *Aurantisolimonas haloimpatiens*, has been identified and is known for NO_3^- reduction (Liu et al. 2018).

During the experiment, the relative abundance of *Bradyrhizobium* (Ormeño-Orrillo and Martínez-Romero 2019) increased significantly in CP but not in FP, which might suggest that the flood still affected *Bradyrhizobium* relative abundance. The N-fixing genus *Bradyrhizobium* is also linked to denitrification processes (Gao et al. 2021), with some species capable of complete denitrification and others associated with incomplete denitrification (Saeki et al. 2017).

The most abundant genus at our study site, *Flavobacterium*, is found in riparian areas (Chi et al. 2021). Some *Flavobacterium* species can oxidize carbohydrates (Bernardet and Bowman 2015), reduce NO_3^- to NO_2^- (Zhang et al. 2006), and one *Flavobacterium* species is capable of complete denitrification (Horn et al. 2005, Pishgar et al. 2019). It has been shown that *Flavobacterium* is an N_2O-producing facultative aerobe (Pishgar et al. 2019), and sequencing results showed that with flooding, the abundance of *Flavobacterium* decreased, though not significantly. Also, *Flavobacterium* relative abundance was higher in habitats with greater NO_3^- concentrations.

We analysed the N-mediated n-damo process, an N-cycle process linked to the C cycle, involving the anaerobic bacterium Candidatus *Methylomirabilis oxyfera*. Candidatus *Methylomirabilis oxyfera* reduces NO_2^- to N_2 without N_2O reductase, producing oxygen for CH_4 oxidation (Ettwig et al. 2010). N-damo-specific 16S rRNA gene abundance (determined by qPCR) was positively correlated with N_2O emissions in the FP during the flood. However, our results showed that n-damo-specific 16S rRNA gene abundance did not change significantly during or after the flood, and the genus Candidatus *Methylomirabilis* was not found in the sample area.

Alteration of nitrogen-cycle gene abundances and associated N_2O and N_2 fluxes

Our results suggest a slowdown of nitrification in some locations during the flood. N_2O emissions are typically linked to soil NO_3^- availability (Vilain et al. 2010, Pärn et al. 2018), which accumulates in the soil through nitrification. Our findings show a decrease in soil NO_3 concentration and a decrease in the relative abundance of nitrification-associated bacteria *Nitrospira* (sequencing data), which belongs to the *Nitrosomonadaceae* family and is NH_3 oxidizer (Prosser et al. 2014, Yan et al. 2023) and prefers lower soil water content. Additionally, qPCR results revealed that bacterial and COMAMMOX *amoA* abundance decreased during flooding. *Nitrospira*, known for the comammox process (Wang et al. 2019), decreased in both plots, but the decrease was greater in FP. However, sequencing data showed that flooding increased the relative abundance of AOB from *MND1* and *Ellin6067* genera (not significantly). *Ellin6067* is a main nitrifier in aquaculture ponds, and AOB-driven nitrification has been shown to be the primary source of N_2O in those environments (Deng et al. 2024).

Denitrification is an anaerobic four-step process in which NO_3^- is reduced to N_2 (Kleineidam et al. 2025). The *nirK* and *nirS* genes serve as markers and show potential metabolic capacity for the NO_2^- reduction process (Kuypers et al. 2018). We observed a negative correlation between *nirK* and soil NO_3^- concentration during the flood. Microorganisms that complete the final denitrification step, reducing N_2O to N_2, use N_2O reductase *nosZ* clades I

and II (Hallin et al. 2018). Microorganisms possessing *nosZI* genes are more likely to be complete denitrifiers, as they are typically found alongside *nirK* or *nirS* (Graf et al. 2014). Also, nearshore areas have a low N_2O-producing capability due to the dominance of *nosZI*-harbouring bacteria, which are N_2O-reducing microorganisms (Zhao et al. 2022). Interpolation showed that points with higher soil water content acted as weak N_2O sinks. Flooding increased the abundance of *nosZI* and *nosZII*, with *nosZI* positively correlated with soil water content. Additionally, the average soil water content in the FP (except at points 3 and 5) was above 0.6 m^3/m^3, suggesting conditions favourable for complete denitrification (Vilain et al. 2010).

DNRA is an anaerobic process in OM-rich soils (Rütting et al. 2011), but it can be limited by NO_3^- availability (Silver et al. 2001). FP's interpolation, based on qPCR results, showed higher *nrfA* gene abundance than CP during the flood (Fig. S7E). After the flood, the abundance of *nrfA* was positively correlated with NO_3^- reduction (Fig. S5), suggesting DNRA process activity after the flooding experiment.

Flooding positively influenced microorganisms harbouring the *nifH* gene, indicating a potential metabolic capacity for nitrogen fixation. *nifH* abundance (qPCR data) correlated positively with soil water content, and interpolation, based on qPCR results, showed the highest *nifH* gene abundances at the points closest to the water source (Fig. S6F). Sequencing revealed that flooding significantly increased the relative abundance of *Geomonas* (Fig. 11), potentially N_2-fixer (Ormeño-Orrillo and Martínez-Romero 2019, Liu et al. 2023) carrying the *nifH* gene (Liu et al. 2023).

Temporal impacts of flooding on fungal community structure

Similarly to previous studies, we did not see a significant change in the fungal community, but the relative abundance of *Rozellomycota* group GS02, *Coprinellus*, *Melampsoridium*, *Chytridiomycota*, and *Oliveonia*, *Cercomonadida* changed significantly during or after the flood in the FP (Fig. 11).

Flooding significantly increased the relative abundance of GS02 and *Melampsoridium* fungi. Clade GS02, an ectomycorrhizal fungus (EMF) in the *Rozellomycota* (*Cryptomycota*) phylum, has been found in pine stands (Dewi et al. 2016) and near-neutral temperate soils in Europe (Tedersoo et al. 2017b). The *Rozellomycota* group GS02 has been shown to have cellulase activities (Bhosale et al. 2024) important in decomposing soil OM (Daunoras et al. 2024).

Flooding significantly increased the relative abundance of *Melampsoridium* (Fig. 11). *Melampsoridium* is a rust fungus (*M. hiratsukanum*) that colonizes alder species (Hantula et al. 2009) and can impair leaf physiology and photosynthesis, reducing their ability to fix C (Carretero et al. 2011, Gortari et al. 2018). On the other hand, flooding significantly decreased the relative abundance of *Coprinellus and Cercomonadida* genera. *Coprinellus* has been identified under aerobic conditions and has been shown to be affected by floods (Tian et al. 2015).

The relative abundance of soil saprotroph genera *Oliveonia* (Trofymow et al. 2020) and *Chytridiomycota* decreased significantly after the flood. *Chytridiomycota* are primarily aquatic fungi that can grow on organic material in soils (Barr 2001), and some are able to use NO_3^- as a sole source of nitrogen (Digby et al. 2010).

The relative abundance of *Cortinarius* increased with flooding as soil NO_3^- levels declined. This nitrophobic genus (Lilleskov et al. 2002, Bashian-Victoroff et al. 2025) is found in flooded areas (Sumorok et al. 2008) and wetlands with low soil N availability (Filippova and Thormann 2014, Aučina et al. 2019). The flood increased slightly the relative abundance of genera *Naucoria* and *Russula*, both mycorrhizal associates of alder roots (Moreau 2005). It also increased *Tomentella* abundance, a common genus in the alder microbiome (Schwob et al. 2017, Fuller et al. 2023). Alders form symbiotic relationships with EMF and AMF, which aid nutrient and water uptake and enhance resilience to environmental stress (Fuller et al. 2023).

The most abundant AMF families at the study site were *Claroideoglomeraceae* and *Archaeosporaceae*. During the flood, the relative abundance of the family *Acaulosporaceae* increased significantly (Fig. 11). This family occurs in several different habitats, like tropical forests (Leal et al. 2013), is stress-tolerant (Chagnon et al. 2013) and prefers acidic soils with low soil bulk density and higher N content (Veresoglou et al. 2013, Davison et al. 2021). Flooding and high soil water content can increase bulk density, and fine-textured soils, like the clay soils in this study, are prone to deformation and compaction (Saffih-Hdadi et al. 2009).

Conclusions

Microbiome studies are essential for understanding how soil communities respond and adapt to climate change, particularly in regions where flooding is expected to increase. The average temperature during the experiment ranged from 19.9 ± 2.1°C, and the flood plot was significantly higher in soil moisture. Mid-growing-season flooding significantly impacted soil microbial communities (Fig. 11), particularly the C and N cycles and GHG fluxes. The first hypothesis was partially supported, as bacterial diversity declined during the flood, whereas fungal diversity did not significantly change during or after the flood, confirming its resistance to short-term environmental changes. Among AMF, only *Acaulosporaceae* abundance increased significantly, reinforcing also AMF's resilience to flooding. The second hypothesis proposed that changes in the microbiome are responsible for decreases in N_2O emissions and increases in CH_4 emissions after flooding. We saw that soil water content fluctuations led to CH_4 consumption and emission in FP, favouring n-damo bacteria. The n-damo gene was also positively correlated with soil N_2O emission; however, the genus Candidatus *Methylomirabilis*, which could carry out anaerobic methane oxidation with nitrite reduction, was not detected. The *pmoA* gene, linked to methanotrophic activity, was more abundant in FP, aligning with areas of high CH_4 oxidation. Also, *mcrA* gene was not detected in the samples. Methanogens are anaerobic and most likelely more abundant in deeper layers, or the flooding period may not have been long enough to create favourable conditions. Lower soil water content at N_2O emission spots suggested nitrification as the primary N_2O source. Second hypothesis was therefore partially correct as we saw that flooding created N_2O and CH_4 emission hot spots, but the emissions were influenced by soil water content and microtopography. The third hypothesis was also partially true, as soil water content was positively correlated with bacterial *amoA*, while the relative abundances of nitrifiers *MND1* and *Ellin6067* increased. On the other hand, the comammox process decreased with flooding as the relative abundance of *Nitrospira* and COMAMMOX *amoA* gene copies decreased. Flooding positively influenced alder-associated fungi (*Naucoria*, *Russula*, and *Tomentella*) and N_2-fixing bacteria (*Bradyrhizobium* and *Geomonas*), with *nifH* gene abundance highest at points closest to the water source.

The pulsing nature and duration of short-term flooding and microtopography influenced soil microbial communities and processes, underscoring the intricate interplay between hydrology, soil microbiology, and GHG fluxes. This study highlights the need

for further experiments to examine microgradients between alder roots and bulk soil.

Author contributions

Kristel Reiss (Data curation, Formal Analysis, Investigation, Methodology, Visualization, Writing – original draft, Writing – review & editing), Ülo Mander (Conceptualization, Funding acquisition, Supervision, Writing – review & editing), Maarja Öpik (Formal Analysis, Funding acquisition, Writing – review & editing), Siim-Kaarel Sepp (Formal Analysis, Writing – review & editing), Kärt Kanger (Data curation, Investigation, Methodology, Writing – review & editing), Thomas Schindler (Data curation, Investigation, Writing – review & editing), Kaido Soosaar (Data curation, Writing – review & editing), Mari Pihlatie (Writing – review & editing), Klaus Butterbach-Bahl (Writing – review & editing), Anuliina Putkinen (Writing – review & editing), Ülo Niinemets (Funding acquisition, Writing – review & editing), and Mikk Espenberg (Data curation, Formal Analysis, Investigation, Supervision, Writing – review & editing)

Supplementary data

Supplementary data is available at *FEMSEC Journal* online.

Conflict of interest: The authors declare that they have no conflict of interest.

Funding

This study was supported by the Estonian Research Council (PRG2032, PRG1789, and PUTJD1273), the European Union Horizon program under grant agreement number 101079192 (MLTOM23003R), the European Research Council (ERC) under grant agreement number 101096403 (MLTOM23415R), European Commission under grant agreement number 322603 (8-2/T13006PKTF), and EC Horizon Project GreenFeedBack (101056921).

Data availability

The data underlying this article are available in European Nucleotide Archive at https://www.ebi.ac.uk/ena/browser/home, and can be accessed with the primary accession code PRJEB86668.

References

Adhikari K, Owens PR, Ashworth AJ *et al.* Topographic controls on soil nutrient variations in a silvopasture system. *Agrosyst Geosci Environ* 2018;**1**:1–15. https://doi.org/10.2134/age2018.04.0008.

Annala M, Lehosmaa K, Ahonen S *et al.* Effect of riparian soil moisture on bacterial, fungal and plant communities and microbial decomposition rates in boreal stream-side forests. *Forest Ecol Manag* 2022;**519**:120344. https://doi.org/10.1016/j.foreco.2022.120344.

Antler G, Turchyn AV, Herut B *et al.* Sulfur and oxygen isotope tracing of sulfate driven anaerobic methane oxidation in estuarine sediments. *Estuar Coast Shelf Sci* 2014;**142**:4–11. https://doi.org/10.1016/j.ecss.2014.03.001.

Aosaar J, Varik M, Uri V. Biomass production potential of grey alder (*Alnus incana* (L.) Moench.) in Scandinavia and Eastern Europe:a review. *Biomass Bioenergy* 2012;**45**:11–26. https://doi.org/10.1016/j.biombioe.2012.05.013.

APHA-AWWA-WEF. Standard Methods for the Examination of Water and Wastewater. New York, 2005.

Aučina A, Rudawska M, Wilgan R *et al.* Functional diversity of ectomycorrhizal fungal communities along a peatland–forest gradient. *Pedobiologia* 2019;**74**:15–23.

Bahram M, Anslan S, Hildebrand F *et al.* Newly designed 16S rRNA metabarcoding primers amplify diverse and novel archaeal taxa from the environment. *Environ Microbiol Rep* 2019;**11**:487–94. https://doi.org/10.1111/1758-2229.12684.

Bahram M, Espenberg M, Pärn J *et al.* Structure and function of the soil microbiome underlying N_2O emissions from global wetlands. *Nat Commun* 2022;**13**:1430. https://doi.org/10.1038/s41467-022-29161-3.

Barnett D. david-barnett/microViz:microViz 0.12.5. Zenodo, 2024. https://doi.org/10.5281/zenodo.13763600.

Barr D. Chytridiomycota. In: *Systematics and Evolution: Part A*. Berlin: Springer, 2001, 93–112. https://doi.org/10.1007/978-3-662-10376-0.

Bashian-Victoroff C, Yanai RD, Horton TR *et al.* Nitrogen and phosphorus additions affect fruiting of ectomycorrhizal fungi in a temperate hardwood forest. *Fungal Ecol* 2025;**73**:101388. https://doi.org/10.1016/j.funeco.2024.101388.

Bernardet J-F, Bowman JP. Flavobacterium. In: *Bergey's Manual of Systematics of Archaea and Bacteria*. Hoboken: Wiley, 2015, 1–75.

Bhosale S, Chavan V, Patil N *et al.* Antifungal activity of grape associated bacterial endophytes against pathogenic fungi. *Biologia* 2024;**79**:3409–17. https://doi.org/10.1007/s11756-024-01774-7.

Boetius A, Ravenschlag K, Schubert CJ *et al.* A marine microbial consortium apparently mediating anaerobic oxidation of methane. *Nature* 2000;**407**:623–6. https://doi.org/10.1038/35036572.

Caldwell SL, Laidler JR, Brewer EA *et al.* Anaerobic oxidation of methane: mechanisms, bioenergetics, and the ecology of associated microorganisms. *Environ Sci Technol* 2008;**42**:6791–9. https://doi.org/10.1021/es800120b.

Callahan B. Silva taxonomic training data formatted for DADA2 (Silva version 138.2). Zenodo, 2024. https://doi.org/10.5281/zenodo.14169026.

Callahan BJ, McMurdie PJ, Rosen MJ *et al.* DADA2: high-resolution sample inference from Illumina amplicon data. *Nat Methods* 2016;**13**:581–3. https://doi.org/10.1038/nmeth.3869.

Canfield DE, Thamdrup B, Hansen JW. The anaerobic degradation of organic matter in Danish coastal sediments: iron reduction, manganese reduction, and sulfate reduction. *Geochim Cosmochim Acta* 1993;**57**:3867–83. https://doi.org/10.1016/0016-7037(93)90340-3.

Caporaso JG, Lauber CL, Walters WA *et al.* Global patterns of 16S rRNA diversity at a depth of millions of sequences per sample. *Proc Natl Acad Sci USA* 2011;**108**:4516–22. https://doi.org/10.1073/pnas.1000080107.

Carretero R, Bancal MO, Miralles DJ. Effect of leaf rust (*Puccinia triticina*) on photosynthesis and related processes of leaves in wheat crops grown at two contrasting sites and with different nitrogen levels. *Eur J Agron* 2011;**35**:237–46. https://doi.org/10.1016/j.eja.2011.06.007.

Cavicchioli R, Ripple WJ, Timmis KN *et al.* Scientists' warning to humanity: microorganisms and climate change. *Nat Rev Microbiol* 2019;**17**:569–86. https://doi.org/10.1038/s41579-019-0222-5.

Chagnon P-L, Bradley RL, Maherali H *et al.* A trait-based framework to understand life history of mycorrhizal fungi. *Trends Plant Sci* 2013;**18**:484–91. https://doi.org/10.1016/j.tplants.2013.05.001.

Chen H, Yu F, Shi W. Detection of N_2O-producing fungi in environment using nitrite reductase gene (nirK)-targeting primers. *Fungal Biol* 2016;**120**:1479–92. https://doi.org/10.1016/j.funbio.2016.07.012.

Chi Z, Wang W, Li H *et al.* Soil organic matter and salinity as critical factors affecting the bacterial community and function of *Phragmites australis* dominated riparian and coastal wetlands. *Sci Total Environ* 2021;**762**:143156. https://doi.org/10.1016/j.scitotenv.2020.143156.

Chowdhury TR, Dick RP. Ecology of aerobic methanotrophs in controlling methane fluxes from wetlands. *Appl Soil Ecol* 2013;**65**:8–22. https://doi.org/10.1016/j.apsoil.2012.12.014.

Clemmensen K, Bahr A, Ovaskainen O *et al.* Roots and associated fungi drive long-term carbon sequestration in boreal forest. *Science* 2013;**339**:1615–8. https://doi.org/10.1126/science.1231923.

Clerici N, Weissteiner CJ, Paracchini ML *et al.* Pan-European distribution modelling of stream riparian zones based on multi-source Earth Observation data. *Ecol Indic* 2013;**24**:211–23. https://doi.org/10.1016/j.ecolind.2012.06.002.

Congreves KA, Phan T, Farrell RE. A new look at an old concept: using 15 N_2O isotopomers to understand the relationship between soil moisture and N_2O production pathways. *Soil* 2019;**5**:265–74. https://doi.org/10.5194/soil-5-265-2019.

Cui M, Ma A, Qi H *et al.* Anaerobic oxidation of methane: an "active" microbial process. *MicrobiologyOpen* 2015;**4**:1–11. https://doi.org/10.1002/mbo3.232.

Daunoras J, Kačergius A, Gudiukaitė R. Role of soil microbiota enzymes in soil health and activity changes depending on climate change and the type of soil ecosystem. *Biology* 2024;**13**:85. https://doi.org/10.3390/biology13020085.

Davison J, Moora M, Semchenko M *et al.* Temperature and pH define the realised niche space of arbuscular mycorrhizal fungi. *New Phytol* 2021;**231**:763–76. https://doi.org/10.1111/nph.17240.

Deng M, Yeerken S, Wang Y *et al.* Greenhouse gases emissions from aquaculture ponds: different emission patterns and key microbial processes affected by increased nitrogen loading. *Sci Total Environ* 2024;**926**:172108. https://doi.org/10.1016/j.scitotenv.2024.172108.

Dewi M, Esyanti RR, Aryantha INP. Diversity of suillus fungi from pine (*Pinus merkusii*) stands at various locations in Bandung Area, Indonesia. *Plant Pathol J* 2016;**15**: 95–101.

Diagne N, Ngom M, Djighaly PI *et al.* Roles of arbuscular mycorrhizal fungi on plant growth and performance: importance in biotic and abiotic stressed regulation. *Diversity* 2020;**12**:370. https://doi.org/10.3390/d12100370.

Digby AL, Gleason FH, McGee PA. Some fungi in the Chytridiomycota can assimilate both inorganic and organic sources of nitrogen. *Fungal Ecol* 2010;**3**:261–6. https://doi.org/10.1016/j.funeco.2009.11.002.

Dumbrell AJ, Ashton PD, Aziz N *et al.* Distinct seasonal assemblages of arbuscular mycorrhizal fungi revealed by massively parallel pyrosequencing. *New Phytol* 2011;**190**:794–804. https://doi.org/10.1111/j.1469-8137.2010.03636.x.

Espenberg M, Pille K, Yang B *et al.* Towards an integrated view on microbial CH_4, N_2O and N_2 cycles in brackish coastal marsh soils: a comparative analysis of two sites. *Sci Total Environ* 2024;**918**:170641. https://doi.org/10.1016/j.scitotenv.2024.170641.

Espenberg M, Truu M, Mander Ü *et al.* Differences in microbial community structure and nitrogen cycling in natural and drained tropical peatland soils. *Sci Rep* 2018;**8**:4742. https://doi.org/10.1038/s41598-018-23032-y.

Espenberg M, Truu M, Truu J *et al.* Impact of reed canary grass cultivation and mineral fertilisation on the microbial abundance and genetic potential for methane production in residual peat of an abandoned peat extraction area. *PLoS One* 2016;**11**:e0163864. https://doi.org/10.1371/journal.pone.0163864.

Esri. *IDW (Geostatistical Analyst)*. Noida, 2025. https://pro.arcgis.com/en/pro-app/latest/tool-reference/geostatistical-analyst/idw.htm(26 January 2025, date last accessed).

Ettwig KF, van Alen T, van de Pas-Schoonen KT *et al.* Enrichment and molecular detection of denitrifying methanotrophic bacteria of the NC10 phylum. *Appl Environ Microbiol* 2009;**75**:3656–62. https://doi.org/10.1128/AEM.00067-09.

,Ettwig KF, ,Butler MK, ,Le Paslier D *et al.*. Nitrite-driven anaerobic methane oxidation by oxygenic bacteria. *Nature* 2010;**464**:543–548. https://doi.org/10.1038/nature08883

Fang Y, Gundersen P, Zhang W *et al.* Soil–atmosphere exchange of N_2O, CO_2 and CH_4 along a slope of an evergreen broad-leaved forest in southern China. *Plant Soil* 2009;**319**:37–48. https://doi.org/10.1007/s11104-008-9847-2.

Filippova N, Thormann M. Communities of larger fungi of ombrotrophic bogs in West Siberia. *Mires Peat* 2014;**14**:1–22.

Franche C, Lindström K, Elmerich C. Nitrogen-fixing bacteria associated with leguminous and non-leguminous plants. *Plant Soil* 2009;**321**:35–59. https://doi.org/10.1007/s11104-008-9833-8.

Fuller E, Germaine KJ, Rathore DS. The good, the bad, and the useable microbes within the common alder (*Alnus glutinosa*) microbiome—potential bio-agents to combat alder dieback. *Microorganisms* 2023;**11**:2187. https://doi.org/10.3390/microorganisms11092187.

Furtak K, Wolińska A. The impact of extreme weather events as a consequence of climate change on the soil moisture and on the quality of the soil environment and agriculture–a review. *Catena* 2023;**231**:107378. https://doi.org/10.1016/j.catena.2023.107378.

Gao Y, Mania D, Mousavi SA *et al.* Competition for electrons favours N_2O reduction in denitrifying *Bradyrhizobium* isolates. *Environ Microbiol* 2021;**23**:2244–59. https://doi.org/10.1111/1462-2920.15404.

Ghanbary E, Tabari M, González E *et al.* Morphophysiological responses of *Alnus subcordata* (L.) seedlings to permanent flooding and partial submersion. *Int J Environ Sci* 2012;**2**:1211.

Gill CJ. The ecological significance of adventitious rooting as a response to flooding in woody species, with special reference to *Alnus glutinosa* (L.) Gaertn. *Flora* 1975;**164**:85–97. https://doi.org/10.1016/S0367-2530(17)31790-5.

Gortari F, Guiamet JJ, Graciano C. Plant–pathogen interactions: leaf physiology alterations in poplars infected with rust (*Melampsora medusae*). *Tree Physiol* 2018;**38**:925–35. https://doi.org/10.1093/treephys/tpx174.

Graça J, Daly K, Bondi G *et al.* Drainage class and soil phosphorus availability shape microbial communities in Irish grasslands. *Eur J Soil Biol* 2021;**104**:103297.

Graf DR, Jones CM, Hallin S. Intergenomic comparisons highlight modularity of the denitrification pathway and underpin the importance of community structure for N_2O emissions. *PLoS One* 2014;**9**:e114118. https://doi.org/10.1371/journal.pone.0114118.

Graziano MP, Deguire AK, Surasinghe TD. Riparian buffers as a critical landscape feature: insights for riverscape conservation and policy renovations. *Diversity* 2022;**14**:172. https://doi.org/10.3390/d14030172.

Guerrero-Cruz S, Vaksmaa A, Horn MA *et al.* Methanotrophs: discoveries, environmental relevance, and a perspective on current and future applications. *Front Microbiol* 2021;**12**:678057. https://doi.org/10.3389/fmicb.2021.678057.

Gui H, Gao Y, Wang Z *et al.* Arbuscular mycorrhizal fungi potentially regulate N_2O emissions from agricultural soils via altered expression of denitrification genes. *Sci Total Environ* 2021;**774**:145133. https://doi.org/10.1016/j.scitotenv.2021.145133.

Guo J, Feng H, Peng C *et al.* Global climate change increases terrestrial soil CH_4 emissions. *Global Biogeochem Cyc* 2023;**37**:e2021GB007255. https://doi.org/10.1029/2021GB007255.

Hallin S, Lindgren P-E. PCR detection of genes encoding nitrite reductase in denitrifying bacteria. *Appl Environ Microbiol* 1999;**65**:1652–7. https://doi.org/10.1128/AEM.65.4.1652-1657.1999.

Hallin S, Philippot L, Löffler FE *et al.* Genomics and ecology of novel N_2O-reducing microorganisms. *Trends Microbiol* 2018;**26**:43–55. https://doi.org/10.1016/j.tim.2017.07.003.

Hantula J, Kurkela T, Hendry S *et al.* Morphological measurements and ITS sequences show that the new alder rust in Europe is conspecific with *Melampsoridium hiratsukanum* in eastern Asia. *Mycologia* 2009;**101**:622–31. https://doi.org/10.3852/07-164.

Harrell FE., Jr Package 'hmisc'. CRAN, 2019, 235–6.

Harris E, Diaz-Pines E, Stoll E *et al.* Denitrifying pathways dominate nitrous oxide emissions from managed grassland during drought and rewetting. *Sci Adv* 2021;**7**:eabb7118. https://doi.org/10.1126/sciadv.abb7118.

Hefting M, Clement J-C, Dowrick D *et al.* Water table elevation controls on soil nitrogen cycling in riparian wetlands along a European climatic gradient. *Biogeochemistry* 2004;**67**:113–34. https://doi.org/10.1023/B:BIOG.0000015320.69868.33.

Henry S, Bru D, Stres B *et al.* Quantitative detection of the nosZ gene, encoding nitrous oxide reductase, and comparison of the abundances of 16S rRNA, narG, nirK, and nosZ genes in soils. *Appl Environ Microbiol* 2006;**72**:5181–9. https://doi.org/10.1128/AEM.00231-06.

Hernandez ME, Mitsch WJ. Influence of hydrologic pulses, flooding frequency, and vegetation on nitrous oxide emissions from created riparian marshes. *Wetlands* 2006;**26**:862–77. https://doi.org/10.1672/0277-5212(2006)26%5b862:IOHPFF%5d2.0.CO;2.

Horn MA, Ihssen J, Matthies C *et al. Dechloromonas denitrificans* sp. nov., *Flavobacterium denitrificans* sp. nov., *Paenibacillus anaericanus* sp. nov. and *Paenibacillus terrae* strain MH72, N_2O-producing bacteria isolated from the gut of the earthworm *Aporrectodea caliginosa*. *Int J Syst Evol Microbiol* 2005;**55**:1255–65. https://doi.org/10.1099/ijs.0.63484-0.

Huaisong W, Rui G, Yibo T *et al.* Arbuscular mycorrhizal fungi reduce ammonia emissions under different land-use types in agro-pastoral areas. *Pedosphere* 2024;**34**:497–507.

Hutchins DA, Jansson JK, Remais JV *et al.* Climate change microbiology—problems and perspectives. *Nat Rev Microbiol* 2019;**17**:391–6. https://doi.org/10.1038/s41579-019-0178-5.

Ihrmark K, Bödeker IT, Cruz-Martinez K *et al.* New primers to amplify the fungal ITS2 region–evaluation by 454-sequencing of artificial and natural communities. *FEMS Microbiol Ecol* 2012;**82**:666–77. https://doi.org/10.1111/j.1574-6941.2012.01437.x.

IPCC, 2021: summary for policymakers. In: Masson Delmotte V., Zhai P., Pirani A. *et al.* (eds), *Climate Change 2021: The Physical Science Basis. Contribution of Working Group Ito the Sixth Assessment Report of the Intergovernmental Panel on Climate Change*. Cambridge, New York: Cambridge University Press, 2021, 3–32. https://doi.org/10.1017/9781009157896.001.

Itoh H, Xu Z, Masuda Y *et al. Geomonas silvestris* sp. nov., *Geomonas paludis* sp. nov. and *Geomonas limicola* sp. nov., isolated from terrestrial environments, and emended description of the genus *Geomonas*. *Int J Syst Evol Microbiol* 2021;**71**:004607. https://doi.org/10.1099/ijsem.0.004607.

Jacinthe P, Bills J, Tedesco L *et al.* Nitrous oxide emission from riparian buffers in relation to vegetation and flood frequency. *J Environ Qual* 2012;**41**:95–105. https://doi.org/10.2134/jeq2011.0308.

Jacinthe P. Carbon dioxide and methane fluxes in variably-flooded riparian forests. *Geoderma* 2015;**241-242**:41–50. https://doi.org/10.1016/j.geoderma.2014.10.013.

Jiang Z-M, Mou T, Sun Y *et al.* Environmental distribution and genomic characteristics of *Solirubrobacter*, with proposal of two novel species. *Front Microbiol* 2023;**14**:1267771. https://doi.org/10.3389/fmicb.2023.1267771.

Johansson T. Site index curves for common alder and grey alder growing on different types of forest soil in Sweden. *Scand J For Res* 1999;**14**:441–53. https://doi.org/10.1080/02827589950154140.

Jones CM, Graf DR, Bru D *et al.* The unaccounted yet abundant nitrous oxide-reducing microbial community: a potential nitrous oxide sink. *ISME J* 2013;**7**:417–26. https://doi.org/10.1038/ismej.2012.125.

Josse J, Husson F. missMDA: a package for handling missing values in multivariate data analysis. *J Stat Soft* 2016;**70**:1–31. https://doi.org/10.18637/jss.v070.i01.

Kandeler E, Deiglmayr K, Tscherko D *et al.* Abundance of narG, nirS, nirK, and nosZ genes of denitrifying bacteria during primary successions of a glacier foreland. *Appl Environ Microbiol* 2006;**72**:5957–62. https://doi.org/10.1128/AEM.00439-06.

Kassambara A. ggpubr: "ggplot2" based publication ready plots. CRAN, 2023b. https://doi.org/10.32614/CRAN.package.ggpubr.

Kassambara A. Rstatix: pipe-friendly framework for basic statistical tests. CRAN, 2023a.

Kleineidam K, Böttcher J, Butterbach-Bahl K *et al.* Denitrification in agricultural soils–integrated control and modelling at various scales (DASIM). *Biol Fertil Soils* 2025;**61**:1–14.

Koch H, van Kessel MA, Lücker S. Complete nitrification: insights into the ecophysiology of comammox *Nitrospira*. *Appl Microbiol Biotechnol* 2019;**103**:177–89. https://doi.org/10.1007/s00253-018-9486-3.

Kohout P, Sudová R, Janoušková M *et al.* Comparison of commonly used primer sets for evaluating arbuscular mycorrhizal fungal communities: is there a universal solution? *Soil Biol Biochem* 2014;**68**:482–93. https://doi.org/10.1016/j.soilbio.2013.08.027.

Kõljalg U, Nilsson HR, Schigel D *et al.* The taxon hypothesis paradigm—on the unambiguous detection and communication of taxa. *Microorganisms* 2020;**8**:1910. https://doi.org/10.3390/microorganisms8121910

Kubartová A, Ranger J, Berthelin J *et al.* Diversity and decomposing ability of saprophytic fungi from temperate forest litter. *Microb Ecol* 2009;**58**:98–107. https://doi.org/10.1007/s00248-008-9458-8.

Kuypers MM, Marchant HK, Kartal B. The microbial nitrogen-cycling network. *Nat Rev Microbiol* 2018;**16**:263–76. https://doi.org/10.1038/nrmicro.2018.9.

Land and Spatial Development Board. *Estonian Topographic Database*. Tallinn, 2025. https://geoportaal.maaamet.ee/eng/spatial-data/estonian-topographic-database-p305.html(26 January 2025, date last accessed).

Le Mer J, Roger P. Production, oxidation, emission and consumption of methane by soils: a review. *Eur J Soil Biol* 2001;**37**:25–50. https://doi.org/10.1016/S1164-5563(01)01067-6.

Leal PL, Siqueira JO, Stuermer SL. Switch of tropical Amazon forest to pasture affects taxonomic composition but not species abundance and diversity of arbuscular mycorrhizal fungal community. *Appl Soil Ecol* 2013;**71**:72–80. https://doi.org/10.1016/j.apsoil.2013.05.010.

Lee J, Lee S, Young JPW. Improved PCR primers for the detection and identification of arbuscular mycorrhizal fungi. *FEMS Microbiol Ecol* 2008;**65**:339–49. https://doi.org/10.1111/j.1574-6941.2008.00531.x.

Li J, Pei J, Fang C *et al.* Opposing seasonal temperature dependencies of CO_2 and CH_4 emissions from wetlands. *Global Change Biol* 2023;**29**:1133–43. https://doi.org/10.1111/gcb.16528.

Lidman F, Boily Å, Laudon H *et al.* From soil water to surface water–how the riparian zone controls element transport from a boreal forest to a stream. *Biogeosciences* 2017;**14**:3001–14. https://doi.org/10.5194/bg-14-3001-2017.

Lilleskov EA, Fahey TJ, Horton TR *et al.* Belowground ectomycorrhizal fungal community change over a nitrogen deposition gradient in Alaska. *Ecology* 2002;**83**:104–15. https://doi.org/10.1890/0012-9658(2002)083%5b0104:BEFCCO%5d2.0.CO;2.

Lin Z, Shi L, Wei X *et al.* Soil properties and fungal community jointly explain N_2O emissions following N and P enrichment in an alpine meadow. *Environ Pollut* 2024;**344**:123344. https://doi.org/10.1016/j.envpol.2024.123344.

Liu G-H, Yang S, Han S *et al.* Nitrogen fixation and transcriptome of a new diazotrophic Geomonas from paddy soils. *mBio* 2023;**14**:e02150–23. https://doi.org/10.1128/mbio.02150-23.

Liu M-J, Jin C-Z, Asem MD *et al.* *Aurantisolimonas haloimpatiens* gen. nov., sp. nov., a bacterium isolated from soil. *Int J Syst Evol Microbiol* 2018;**68**:1552–9. https://doi.org/10.1099/ijsem.0.002709.

Lõhmus K, Mander Ü, Tullus H *et al.* Productivity, buffering capacity and resources of grey alder forests in Estonia. In: *Proceedings of the Short rotation willow coppice for renewable energy and improved environment conference*. Uppsala: Swedish University of Agricultural Sciences, Uppsala, 1996, 95–105.

Louca S, Parfrey LW, Doebeli M. Decoupling function and taxonomy in the global ocean microbiome. *Science* 2016;**353**:1272–7. https://doi.org/10.1126/science.aaf4507.

Lyu C, Li X, Yuan P *et al.* Nitrogen retention effect of riparian zones in agricultural areas: a meta-analysis. *J Clean Prod* 2021;**315**:128143. https://doi.org/10.1016/j.jclepro.2021.128143.

Mander Ü, Dotro G, Ebie Y *et al.* Greenhouse gas emission in constructed wetlands for wastewater treatment: a review. *Ecol Eng* 2014;**66**:19–35. https://doi.org/10.1016/j.ecoleng.2013.12.006.

Mander Ü, Krasnova A, Schindler T *et al.* Long-term dynamics of soil, tree stem and ecosystem methane fluxes in a riparian forest. *Sci Total Environ* 2022;**809**:151723. https://doi.org/10.1016/j.scitotenv.2021.151723.

Mander Ü, Maddison M, Soosaar K *et al.* The impact of a pulsing groundwater table on greenhouse gas emissions in riparian grey alder stands. *Environ Sci Pollut Res* 2015;**22**:2360–71. https://doi.org/10.1007/s11356-014-3427-1.

Mander Ü, Kuusemets V, Lõhmus K, *et al.*. Efficiency and dimensioning of riparian buffer zones in agricultural catchments. *Ecological engineering* 1997;**8**:299–324. https://doi.org/10.1016/S0925-8574(97)00025-6

Mania D, Heylen K, van Spanning RJ *et al.* The nitrate-ammonifying and nosZ-carrying bacterium *Bacillus vireti* is a potent source and sink for nitric and nitrous oxide under high nitrate conditions. *Environ Microbiol* 2014;**16**:3196–210. https://doi.org/10.1111/1462-2920.12478.

Martin M. Cutadapt removes adapter sequences from high-throughput sequencing reads. *EMBnet j* 2011;**17**:10–2. https://doi.org/10.14806/ej.17.1.200.

McDonald M, Galwey N, Colmer T. Similarity and diversity in adventitious root anatomy as related to root aeration among a range of wetland and dryland grass species. *Plant Cell Environ* 2002;**25**:441–51. https://doi.org/10.1046/j.0016-8025.2001.00817.x.

McMurdie PJ, Holmes S. phyloseq: an R package for reproducible interactive analysis and graphics of microbiome census data. *PLoS One* 2013;**8**:e61217. https://doi.org/10.1371/journal.pone.0061217.

Miller SP. Arbuscular mycorrhizal colonization of semi-aquatic grasses along a wide hydrologic gradient. *New Phytol* 2000;**145**:145–55. https://doi.org/10.1046/j.1469-8137.2000.00566.x.

Moreau P-A. A nomenclatural revision of the genus Alnicola (Cortinariaceae). *Fungal Divers* 2005;**20**:121–55.

Mothapo N, Chen H, Cubeta MA *et al.* Phylogenetic, taxonomic and functional diversity of fungal denitrifiers and associated N_2O production efficacy. *Soil Biol Biochem* 2015;**83**:160–75. https://doi.org/10.1016/j.soilbio.2015.02.001.

Naiman RJ, Decamps H, McClain ME. *Riparia: Ecology, Conservation, and Management of Streamside Communities*. Amsterdam: Elsevier, 2010.

Okiobe ST, Pirhofer-Walzl K, Leifheit EF *et al.* Proximal and distal mechanisms through which arbuscular mycorrhizal associations alter terrestrial denitrification. *Plant Soil* 2022;**476**:315–36. https://doi.org/10.1007/s11104-022-05534-x.

Oksanen J, Simpson GL, Blanchet FG *et al.* vegan: Community Ecology Package. CRAN, 2022.

Oksanen J. vegan: Ecological Diversity. CRAN, 2024.

Oni OE, Friedrich MW. Metal oxide reduction linked to anaerobic methane oxidation. *Trends Microbiol* 2017;**25**:88–90. https://doi.org/10.1016/j.tim.2016.12.001.

Öpik M, Vanatoa A, Vanatoa E *et al.* The online database MaarjAM reveals global and ecosystemic distribution patterns in arbuscular mycorrhizal fungi (Glomeromycota). *New Phytol* 2010;**188**:223–41.

Ormeño-Orrillo E, Martínez-Romero E. A genomotaxonomy view of the *Bradyrhizobium* genus. *Front Microbiol* 2019;**10**:1334. https://doi.org/10.3389/fmicb.2019.01334.

Orwin KH, Kirschbaum MU, St John MG *et al.* Organic nutrient uptake by mycorrhizal fungi enhances ecosystem carbon storage: a model-based assessment. *Ecol Lett* 2011;**14**:493–502. https://doi.org/10.1111/j.1461-0248.2011.01611.x.

Pärn J, Verhoeven JT, Butterbach-Bahl K *et al.* Nitrogen-rich organic soils under warm well-drained conditions are global nitrous oxide emission hotspots. *Nat Commun* 2018;**9**:1–8.

Peter S, Rechsteiner R, Lehmann MF *et al.* Nitrate removal in a restored riparian groundwater system: functioning and importance of individual riparian zones. *Biogeosciences* 2012;**9**:4295–307. https://doi.org/10.5194/bg-9-4295-2012.

Petersen CR, Jovanovic N, Grenfell M. The effectiveness of riparian zones in mitigating water quality impacts in an agriculturally dominated river system in South Africa. *Afr J Aquat Sci* 2020;**45**:336–49. https://doi.org/10.2989/16085914.2019.1685451.

Pinay G, Ruffinoni C, Fabre A. Nitrogen cycling in two riparian forest soils under different geomorphic conditions. *Biogeochemistry* 1995;**30**:9–29. https://doi.org/10.1007/BF02181038.

Pishgar R, Dominic JA, Sheng Z *et al.* Denitrification performance and microbial versatility in response to different selection pressures. *Bioresour Technol* 2019;**281**:72–83. https://doi.org/10.1016/j.biortech.2019.02.061.

Prosser JI, Head IM, Stein LY. The family nitrosomonadaceae. In: *The Prokaryotes: Alphaproteobacteria and Betaproteobacteria*. Berlin, Heidelberg: Springer, 2014, 901–18. https://doi.org/10.1007/978-3-642-30197-1.

Qiu Q, Bender SF, Mgelwa AS *et al.* Arbuscular mycorrhizal fungi mitigate soil nitrogen and phosphorus losses: a meta-analysis. *Sci Total Environ* 2022;**807**:150857. https://doi.org/10.1016/j.scitotenv.2021.150857.

Quast C, Pruesse E, Yilmaz P *et al.* The SILVA ribosomal RNA gene database project: improved data processing and web-based tools. *Nucleic Acids Res* 2013;**41**:D590–6. https://doi.org/10.1093/nar/gks1219.

R Core Team. *R: A Language and Environment for Statistical Computing*. Vienna: R Foundation for Statistical Computing, 2023.

Reed SC, Cleveland CC, Townsend AR. Functional ecology of free-living nitrogen fixation: a contemporary perspective. *Annu Rev Ecol Evol Syst* 2011;**42**:489–512. https://doi.org/10.1146/annurev-ecolsys-102710-145034.

Riis T, Kelly-Quinn M, Aguiar FC *et al.* Global overview of ecosystem services provided by riparian vegetation. *Bioscience* 2020;**70**:501–14. https://doi.org/10.1093/biosci/biaa041.

Rotthauwe J-H, Witzel K-P, Liesack W. The ammonia monooxygenase structural gene amoA as a functional marker: molecular fine-scale analysis of natural ammonia-oxidizing populations. *Appl Environ Microbiol* 1997;**63**:4704–12. https://doi.org/10.1128/aem.63.12.4704-4712.1997.

Rütting T, Boeckx P, Müller C *et al.* Assessment of the importance of dissimilatory nitrate reduction to ammonium for the terrestrial nitrogen cycle. *Biogeosciences* 2011;**8**:1779–91.

Saeki Y, Nakamura M, Mason MLT *et al.* Effect of flooding and the nosZ gene in bradyrhizobia on bradyrhizobial community structure in the soil. *Microb Environ* 2017;**32**:154–63. https://doi.org/10.1264/jsme2.ME16132.

Saffih-Hdadi K, Défossez P, Richard G *et al.* A method for predicting soil susceptibility to the compaction of surface layers as a function of water content and bulk density. *Soil Tillage Res* 2009;**105**:96–103. https://doi.org/10.1016/j.still.2009.05.012.

Sarneel JM, Hefting MM, Kowalchuk GA *et al.* Alternative transient states and slow plant community responses after changed flooding regimes. *Global Change Biol* 2019;**25**:1358–67. https://doi.org/10.1111/gcb.14569.

Schimel JP, Gulledge JM, Clein-Curley JS *et al.* Moisture effects on microbial activity and community structure in decomposing birch litter in the Alaskan taiga. *Soil Biol Biochem* 1999;**31**:831–8. https://doi.org/10.1016/S0038-0717(98)00182-5.

Schindler T, Mander Ü, Machacova K *et al.* Short-term flooding increases CH_4 and N_2O emissions from trees in a riparian forest soil-stem continuum. *Sci Rep* 2020;**10**:3204. https://doi.org/10.1038/s41598-020-60058-7.

Schwob G, Roy M, Manzi S *et al.* Green alder (*Alnus viridis*) encroachment shapes microbial communities in subalpine soils and impacts its bacterial or fungal symbionts differently. *Environ Microbiol* 2017;**19**:3235–50. https://doi.org/10.1111/1462-2920.13818.

Sellstedt A, Richau KH. Aspects of nitrogen-fixing Actinobacteria, in particular free-living and symbiotic Frankia. *FEMS Microbiol Lett* 2013;**342**:179–86. https://doi.org/10.1111/1574-6968.12116.

Shen R, Lan Z, Rinklebe J, *et al.*. Flooding variations affect soil bacterial communities at the spatial and inter-annual scales. *Science of the Total Environment* 2021;**759**:143471.

Shoun H, Fushinobu S, Jiang L *et al.* Fungal denitrification and nitric oxide reductase cytochrome P450nor. *Phil Trans R Soc B* 2012;**367**:1186–94. https://doi.org/10.1098/rstb.2011.0335.

Silver WL, Herman DJ, Firestone MK. Dissimilatory nitrate reduction to ammonium in upland tropical forest soils. *Ecology* 2001;**82**:2410–6. https://doi.org/10.1890/0012-9658(2001)082%5b2410:DNRTAI%5d2.0.CO;2.

Singleton DR, Furlong MA, Peacock AD *et al. Solirubrobacter pauli* gen. nov., sp. nov., a mesophilic bacterium within the Rubrobacteridae related to common soil clones. *Int J Syst Evol Microbiol* 2003;**53**:485–90. https://doi.org/10.1099/ijs.0.02438-0.

Soosaar K, Mander Ü, Maddison M *et al.* Dynamics of gaseous nitrogen and carbon fluxes in riparian alder forests. *Ecol Eng* 2011;**37**:40–53. https://doi.org/10.1016/j.ecoleng.2010.07.025.

Sumorok B, Kosiński K, Michalska-Hejduk D *et al.* Distribution of ectomycorrhizal fungi in periodically inundated plant communities on the Pilica River floodplain. *Ecohydrol Hydrobiol* 2008;**8**:401–10. https://doi.org/10.2478/v10104-009-0032-x.

Takeuchi J. Habitat segregation of a functional gene encoding nitrate ammonification in estuarine sediments. *Geomicrobiol J* 2006;**23**:75–87. https://doi.org/10.1080/01490450500533866.

Tedersoo L, Bahram M, Puusepp R *et al.* Novel soil-inhabiting clades fill gaps in the fungal tree of life. *Microbiome* 2017;**5**:1–10. https://doi.org/10.1186/s40168-017-0259-5.

Tian W, Bi Y, Zeng W *et al.* Diversity of endophytic fungi of *Myricaria laxiflora* grown under pre-and post-flooding conditions. *Genet Mol Res* 2015;**14**:10849–62. https://doi.org/10.4238/2015.September.9.23.

Tolkkinen MJ, Heino J, Ahonen SH *et al.* Streams and riparian forests depend on each other: a review with a special focus on microbes. *Forest Ecol Manag* 2020;**462**:117962. https://doi.org/10.1016/j.foreco.2020.117962.

Tourna M, Freitag TE, Nicol GW *et al.* Growth, activity and temperature responses of ammonia-oxidizing archaea and bacteria in soil microcosms. *Environ Microbiol* 2008;**10**:1357–64. https://doi.org/10.1111/j.1462-2920.2007.01563.x.

Treseder KK, Lennon JT. Fungal traits that drive ecosystem dynamics on land. *Microbiol Mol Biol Rev* 2015;**79**:243–62. https://doi.org/10.1128/MMBR.00001-15.

Trofymow J, Shay P-E, Myrholm CL *et al.* Fungi associated with tree species at an Alberta oil sands reclamation area, as determined by sporocarp assessments and high-throughput DNA sequencing. *Appl Soil Ecol* 2020;**147**:103359. https://doi.org/10.1016/j.apsoil.2019.09.009.

Ueda T, Suga Y, Yahiro N *et al.* Remarkable N_2-fixing bacterial diversity detected in rice roots by molecular evolutionary analysis of nifH gene sequences. *J Bacteriol* 1995;**177**:1414–7. https://doi.org/10.1128/jb.177.5.1414-1417.1995.

Unger IM, Kennedy AC, Muzika R-M. Flooding effects on soil microbial communities. *Appl Soil Ecol* 2009;**42**:1–8. https://doi.org/10.1016/j.apsoil.2009.01.007.

Uri V, Aosaar J, Varik M *et al.* The dynamics of biomass production, carbon and nitrogen accumulation in grey alder (*Alnus incana* (L.) Moench) chronosequence stands in Estonia. *Forest Ecol Manag* 2014;**327**:106–17. https://doi.org/10.1016/j.foreco.2014.04.040.

van Der Heijden MG, Martin FM, Selosse M-A *et al.* Mycorrhizal ecology and evolution: the past, the present, and the future. *New Phytol* 2015;**205**: 1406–23. https://doi.org/10.1111/nph.13288.

Van Eck W, Lenssen J, Van de Steeg H *et al.* Seasonal dependent effects of flooding on plant species survival and zonation: a comparative study of 10 terrestrial grassland species. *Hydrobiologia* 2006;**565**:59–69. https://doi.org/10.1007/s10750-005-1905-7.

Veresoglou SD, Caruso T, Rillig MC. Modelling the environmental and soil factors that shape the niches of two common arbuscular mycorrhizal fungal families. *Plant Soil* 2013;**368**:507–18. https://doi.org/10.1007/s11104-012-1531-x.

Vilain G, Garnier J, Tallec G *et al.* Effect of slope position and land use on nitrous oxide (N_2O) emissions (Seine Basin, France). *Agric For Meteorol* 2010;**150**:1192–202. https://doi.org/10.1016/j.agrformet.2010.05.004.

Wang L, Zhao M, Du X *et al.* Fungi and cercozoa regulate methane-associated prokaryotes in wetland methane emissions. *Front Microbiol* 2023;**13**:1076610. https://doi.org/10.3389/fmicb.2022.1076610.

Wang M, Huang G, Zhao Z *et al.* Newly designed primer pair revealed dominant and diverse comammox amoA gene in full-scale wastewater treatment plants. *Bioresour Technol* 2018;**270**:580–7. https://doi.org/10.1016/j.biortech.2018.09.089.

Wang X-B, Azarbad H, Leclerc L *et al.* A drying-rewetting cycle imposes more important shifts on soil microbial communities than does reduced precipitation. *mSystems* 2022;**7**:e00247–22. https://doi.org/10.1128/msystems.00247-22.

Wang Y, Huang Y, Qiu Q *et al.* Flooding greatly affects the diversity of arbuscular mycorrhizal fungi communities in the roots of wetland plants. *PLoS One* 2011;**6**:e24512. https://doi.org/10.1371/journal.pone.0024512.

Wang Y, Naumann U, Eddelbuettel D *et al.* mvabund: statistical Methods for analysing multivariate abundance data. CRAN, 2022b.

Wang Z, Cao Y, Zhu-Barker X *et al.* Comammox *Nitrospira* clade B contributes to nitrification in soil. *Soil Biol Biochem* 2019;**135**:392–5. https://doi.org/10.1016/j.soilbio.2019.06.004.

White TJ, Bruns T, Lee S *et al.* Amplification and direct sequencing of fungal ribosomal RNA genes for phylogenetics. *PCR Protoc Guide Methods Appl* 1990;**18**:315–22.

Whiteley JA, Gonzalez A. Biotic nitrogen fixation in the bryosphere is inhibited more by drought than warming. *Oecologia* 2016;**181**:1243–58. https://doi.org/10.1007/s00442-016-3601-x.

Wickham H. *Ggplot2: Elegant Graphics for Data Analysis*. New York: Springer, 2016.

Xia Y, Sun J. Alpha Diversity. *Bioinformatic and Statistical Analysis of Microbiome Data: From Raw Sequences to Advanced Modeling with QIIME 2 and R*. Cham: Springer, 2023, 289–333. https://doi.org/10.1007/978-3-031-21391-5.

Xu Z, Masuda Y, Itoh H *et al.* *Geomonas oryzae* gen. nov., sp. nov., *Geomonas edaphica* sp. nov., *Geomonas ferrireducens* sp. nov., *Geomonas terrae* sp. nov., four ferric-reducing bacteria isolated from paddy soil, and reclassification of three species of the genus *Geobacter* as members of the genus *Geomonas* gen. nov. *Front Microbiol* 2019;**10**:2201.

Xu Z, Masuda Y, Wang X *et al.* Genome-based taxonomic rearrangement of the order Geobacterales including the description of *Geomonas azotofigens* sp. nov. and *Geomonas diazotrophica* sp. nov. *Front Microbiol* 2021;**12**:737531. https://doi.org/10.3389/fmicb.2021.737531.

Yan B, Jiang L, Zhou H *et al.* Performance and microbial community analysis of combined bioreactors in treating high–salinity hydraulic fracturing flowback and produced water. *Bioresour Technol* 2023;**386**:129469. https://doi.org/10.1016/j.biortech.2023.129469.

Yang R, Ji M, Zhang X *et al.* Methane emissions and microbial communities under differing flooding conditions and seasons in littoral wetlands of urban lake. *Environ Res* 2024;**250**:118390. https://doi.org/10.1016/j.envres.2024.118390.

Zhang D-C, Wang H-X, Liu H-C *et al.* *Flavobacterium glaciei* sp. nov., a novel psychrophilic bacterium isolated from the China No. 1 Glacier. *Int J Syst Evol Microbiol* 2006;**56**:2921–5. https://doi.org/10.1099/ijs.0.64564-0.

Zhang L, Zheng J, Han X *et al.* The effect of soil moisture on the response by fungi and bacteria to nitrogen additions for N_2O production. *J For Res* 2021;**32**:2037–45. https://doi.org/10.1007/s11676-020-01262-z.

Zhang X, Jia X, Wu H *et al.* Depression of soil nitrogen fixation by drying soil in a degraded alpine peatland. *Sci Total Environ* 2020;**747**:141084. https://doi.org/10.1016/j.scitotenv.2020.141084.

Zhang Y, Wang F, Xia W *et al.* Anaerobic methane oxidation sustains soil organic carbon accumulation. *Appl Soil Ecol* 2021;**167**:104021. https://doi.org/10.1016/j.apsoil.2021.104021.

Zhang Z, Masuda Y, Xu Z *et al.* Active nitrogen fixation by iron-reducing bacteria in rice paddy soil and its further enhancement by iron application. *Appl Sci* 2023;**13**:8156. https://doi.org/10.3390/app13148156.

Zhao N, Ding H, Zhou X *et al.* Dissimilatory iron-reducing microorganisms: the phylogeny, physiology, applications and outlook. *Crit Rev Environ Sci Technol* 2024;1–26.

Zhao S, Wang X, Pan H *et al.* High N_2O reduction potential by denitrification in the nearshore site of a riparian zone. *Sci Total Environ* 2022;**813**:152458. https://doi.org/10.1016/j.scitotenv.2021.152458.

Received 19 June 2025; **revised** 28 September 2025; **accepted** 21 October 2025